

Review

Analytical Pyrolysis and Mass Spectrometry to Characterise Lignin in Archaeological Wood

Jeannette Jacqueline Lucejko ^{*}, Diego Tamburini , Francesca Modugno, Erika Ribechini  and Maria Perla Colombini

Department of Chemistry and Industrial Chemistry, University of Pisa, via Moruzzi 13, I-56124 Pisa, Italy; tamburinid@si.edu (D.T.); francesca.modugno@unipi.it (F.M.); erika.ribechini@unipi.it (E.R.); maria.perla.colombini@unipi.it (M.P.C.)

* Correspondence: jeannette.lucejko@unipi.it

Abstract: This review describes the capability of analytical pyrolysis-based techniques to provide data on lignin composition and on the chemical alteration undergone by lignin in archaeological wooden objects. Applications of Direct Exposure Mass Spectrometry (DE-MS), Evolved Gas Analysis Mass Spectrometry (EGA-MS), and single and double-shot Pyrolysis-Gas Chromatography/Mass Spectrometry (Py-GC/MS) in archaeological lignin characterisation are described. With comparison to cellulose and hemicelluloses, lignin is generally less prone to most degradation processes affecting archaeological artefacts in burial environments, especially waterlogged ones, which are the most favourable for wood preservation. Nevertheless, lignin also undergoes significant chemical changes. As wood from waterlogged environments is mainly composed of lignin, knowledge of its chemical structure and degradation pathways is fundamental for choosing preventive conservation conditions and for optimising consolidation methods and materials, which directly interact with the residual lignin. Analytical pyrolysis coupled with mass spectrometry, used in several complementary operational modes, can gather information regarding the chemical modifications and the state of preservation of lignin, especially concerning oxidation and depolymerisation phenomena. Several applications to the analysis of wood from archaeological artefacts affected by different conservation problems are presented to showcase the potential of analytical pyrolysis in various scenarios that can be encountered when investigating archaeological waterlogged wood.

Keywords: archaeological wood; lignin; analytical pyrolysis; mass spectrometry



Citation: Lucejko, J.J.; Tamburini, D.; Modugno, F.; Ribechini, E.; Colombini, M.P. Analytical Pyrolysis and Mass Spectrometry to Characterise Lignin in Archaeological Wood. *Appl. Sci.* **2021**, *11*, 240. <https://doi.org/10.3390/app11010240>

Received: 1 December 2020

Accepted: 23 December 2020

Published: 29 December 2020

Publisher's Note: MDPI stays neutral with regard to jurisdictional claims in published maps and institutional affiliations.



Copyright: © 2020 by the authors. Licensee MDPI, Basel, Switzerland. This article is an open access article distributed under the terms and conditions of the Creative Commons Attribution (CC BY) license (<https://creativecommons.org/licenses/by/4.0/>).

1. Introduction

Archaeological wooden artefacts are relatively rare and represent an invaluable source of knowledge on the culture, technology, and everyday activities in ancient human societies, and thus have a high historical significance [1]. Wood is a complex heterogeneous organic material, susceptible to various type of degradation processes, and this makes the preservation of archaeological wood a fundamental challenge for archaeologists and conservators all over the world. The study of wood degradation can be approached in several ways: mechanical, physical, and structural degradation are often evaluated [1], but these aspects are ultimately all related to the chemical degradation of the lignocellulosic matrix constituting wood.

Around 95% of wood is composed by three biopolymers: cellulose, hemicelluloses (together defined as holocellulose), and lignin. The remaining part is made up of organic and inorganic extractives [2]. It is not common for wooden historical artefacts to survive natural degradation in the natural environment due to biodegradation [3], since fungi, bacteria, and insects attack and metabolise wood components [4,5]. Waterlogged conditions favour the preservation of wood, as low temperatures and limited oxygen availability inhibit or decelerate the action of microorganisms [6,7].

Assessing the state of degradation of wood in archaeological artefacts has recently acquired even greater interest due to the severe degradation phenomena observed in consolidated archaeological wooden artefacts exhibited in museum galleries. In fact, it is evident that the degradation processes continue after recovery from the burial environment [8–14]. A range of analytical approaches have been exploited to assess wood decay [12,15–18]. The chemical alteration of archaeological waterlogged wood is often evaluated in terms of the degradation of cellulose and hemicelluloses [7,16,17,19–23]. The loss of polysaccharides can be evaluated using the holocellulose over lignin ratio (H/L), which can be estimated by several techniques and that, when compared with the values obtained for reference sound wood, is considered a proxy for the extent of wood degradation in terms of loss of polysaccharides [15,24]. Less research has been dedicated to the degradation of lignin, due to its relative resilience in the burial environment [25]. Lignin is known to be attacked by white rot fungi [4,6,26,27], but these microorganisms are not active in waterlogged environments [4]. Nevertheless, chemical changes affecting lignin have been in some cases described in archaeological waterlogged wood, and they involve demethylation [28,29], oxidation [10,29–32], and depolymerisation [10,29,33]. Recent studies performed by Py-GC/MS have also shown some minor chemical changes in the structure of the lignin, induced by the burial environment, when fragments of oak wood were buried in the archaeological site for a relatively short time of 10 years [34]. Another recent study, also carried out by Py-GC/MS, reports on the oxidation of lignin observed in ancient papyri. An increase in the relative abundance of some diagnostic compounds with carbonyl and carboxyl functionalities was determined [35]. These phenomena are not effectively described by changes in the H/L ratio. The severe depletion of carbohydrates in waterlogged archaeological wood further prevents the use of the H/L ratio as a chemical parameter to differentiate the extent of wood degradation in different samples or objects, whereas assessing the degradation undergone by the residual lignin has been demonstrated to be an effective discrimination method [8,10,36]. Furthermore, molecular information on lignin is particularly useful to select conservation treatments and consolidation materials: The interactions between the restoration/consolidation materials and the residual lignin can be crucial in determining the stability of the consolidated object.

Analytical techniques based on pyrolysis have proven particularly successful to investigate lignin in archaeological wood [9–11,15,28,30,31,33,34,37–41]. They provide information at a molecular level on complex polymers by studying their pyrolysis products, which are small volatile molecules produced by selective bond cleavage induced by thermal energy [42]. When coupled with gas chromatography (GC) and/or mass spectrometry (MS), thermo-analysis is highly sensitive, requires only small amounts of a sample (usually 10–50 µg), very little sample preparation, and quite short analysis time (from a few minutes to one hour). These technical features are highly desirable in the heritage science field [43].

Lignin pyrolysis products have been identified in pioneering studies [26,44–46], proving that hydroxyphenyl, guaiacyl, and syringyl components of lignin can be distinguished by this technique. Lignin can also be separated from the other wood components before analysis. However, the results obtained on lignin extracted from archaeological wood can be biased by alterations induced by the wet-chemical extraction steps [31,47]. It is thus preferable to pre-treat the sample as little as possible when dealing with archaeological degraded wood, and this requirement is fulfilled by analytical pyrolysis.

When analytical pyrolysis is directly coupled with MS (DE-MS, DT-MS, Py-MS), the time of analysis is very short (a few minutes) and the amount of sample is extremely small (a few grains of milled wood). However, the mass spectra obtained may be very complex as they are the combination of the mass spectra of all the thermal degradation products. Therefore, in some cases, the comparison, classification, and differentiation of the analysed samples are successfully achieved by multivariate analysis of the mass spectral data [38,48–54]. Such analysis can be very useful as a screening step, in order to choose the representative samples for more detailed studies.

Another relatively new approach, which does not involve chromatographic separation, is evolved gas analysis coupled with mass spectrometry (EGA-MS). Based on a thermal degradation occurring over a temperature gradient, this technique provides both thermal and compositional information on the analysed material as well as insights into the interactions between lignin and carbohydrates [55,56]. EGA-MS has been applied to treated and untreated archaeological wood and has enabled the chemical changes undergone by lignin to be clarified [33,36,57].

Recently, direct analysis in real time—mass spectrometry (DART-MS) has been proposed to evaluate the degradation state of archaeological wood [17]. This technique is technically not a pyrolysis-based approach, as wood components are thermally desorbed at ambient pressure. Nevertheless, it shares the same principles of DE-MS, with the advantage that it can be easily coupled to high resolution MS. The use of chemometrics delineates a promising scenario for further application of this technique to archaeological wood analysis.

When chromatographic separation is introduced between pyrolysis and MS analysis (Py-GC/MS), more detailed information is obtained, as the pyrolysis products are separated and singularly identified. However, many lignin pyrolysis products are polar compounds, which are not volatile enough to be effectively separated in a gas chromatographic column. A derivatising agent to be added in situ is useful to improve the chromatographic separation of pyrolysis products bearing carboxylic or alcoholic functionalities [15,58]. Methylating and silylating agents are the most commonly used [15,59]. Hexamethyldisylazane (HMDS) is preferred over tetramethylammonium hydroxide (TMAH) in wood analysis [60], because silylation of phenol groups permits to differentiate them from methoxy groups even after the derivatisation [31]. In addition, trimethylsilylation reduces the reactivity of alcoholic functionalities during pyrolysis, improving the GC-MS detection of the primary lignin pyrolysis products with alcoholic moieties in the side chain such as coniferyl alcohol and sinapyl alcohol [61].

Recent instrumental configurations have led to the development of double-shot and multi-shot Py-GC/MS. A single sample can be exposed to increasing pyrolysis temperatures (shots) and a chromatographic run follows each shot, thus allowing the separation of specific pyrolysis products into different chromatographic runs according to the pyrolysis temperature at which they are formed. Double-shot pyrolysis has been applied to PEG-treated waterlogged wood, enabling the wood and the consolidant to be investigated separately [36].

The aim of this review is to describe the effectiveness of pyrolysis-based techniques (DE-MS, EGA-MS, and single-shot and double-shot Py-GC/MS) to obtain data on the alterations undergone by lignin in archaeological wood. New insights into relevant case studies analysed and partially published during the last ten years at the SCICH (SCIENCE for Cultural Heritage) Laboratory of the University of Pisa (<http://scich.dcci.unipi.it/>) are presented to achieve this aim and to highlight strategies for data interpretation.

2. Case Studies and Archaeological Wood Samples

This section introduces the analysis of several samples from different archaeological sites, which were selected to provide an overview of the variability of results encountered when dealing with archaeological waterlogged wood. The following section focuses on the most significant observations regarding archaeological lignin, which can be drawn when thermal degradation analytical techniques are applied. A description of the samples is presented in the following paragraphs and in Table 1, along with information on analytical techniques used to obtain the data. The instrumental conditions and a more detailed description of the analysed samples can be found in the literature cited.

Table 1. The archaeological wood samples and analytical techniques used to obtain the data discussed. Samples were dried in oven at 40–50 °C for 24 h and milled before analysis.

Archaeological Site	Wood Fragment	Sample Description	Species	Analytical Techniques Applied	Ref
Biskupin (Poland)	Oak 4 Oak 6	4 samples collected from two fragments of wooden parts from the pavement of the ancient settlement. Samples A, B, and C from Oak 4, and one sample from Oak 6.	Oak (<i>Quercus</i> spp.)	Direct Exposure Mass Spectrometry (DE-MS) * Pyrolysis (Hexamethyldisylazane)-Gas Chromatography/Mass Spectrometry (Py(HMDS)-GC/MS) †	[7,53]
Marmotta (Italy)	Pile 2212	7 samples collected from the external part to the core of the pile, following its annual growth rings in groups of five and labelled from A to G.	Oak (<i>Quercus</i> spp.)	DE-MS * Evolved Gas Analysis Mass Spectrometry (EGA-MS) ‡ Py(HMDS)-GC/MS §	[33,62]
Oseberg collection (Norway)	Fragment 185	6 samples from fragment 185 treated with alum in 1905-12. The object had broken up into 6 parts at some point before or after the treatment. Sample 185-1 had the best visual conditions, whereas 185-6 was in the worst condition.	Diffuse porous ring species—probably birch (<i>Betula</i> spp.) or alder (<i>Alnus</i> spp.)	Py(HMDS)-GC/MS §	[8,63]
San Rossore (Italy)	4 shipwrecks	9 samples collected from 4 different shipwrecks.	Beech (<i>Fagus</i> spp.) Elm (<i>Ulmus</i> spp.) Pine (<i>Pinus</i> spp.)	DE-MS *	[53,54]
Żółte (Poland)		5 samples collected from different wooden objects.	Alder (<i>Alnus</i> spp.) Beech (<i>Fagus</i> spp.) Oak (<i>Quercus</i> spp.)	DE-MS *	[37,53]
Lyon (France)	Lyon2 ship	2 samples from the Lyon2 ship (2nd century AD)	Oak (<i>Quercus</i> spp.) Pine (<i>Pinus</i> spp.)	EGA-MS ‡ Single-shot and double-shot Py(HMDS)-GC/MS §	[36]

* Direct Exposure Probe, coupled with a Polaris Q ion trap external ionisation mass spectrometer (Thermo Electron Corporation, USA). The probe program: 0 mA for 20 s, from 0 to 1000 mA in 2 s and 60 s at 1000 mA. † Pyrolyser 5150 CDS Pyroprobe 5000 Series coupled with a 6890 GC and 5973 Mass Selective Detector (Agilent Technologies). Pyrolysis T: 550 °C; HMDS silylating agent for the *in-situ* derivatisation of pyrolysis products. ‡ Multi-Shot Pyrolyzer EGA/Py-3030D (Frontier Lab) coupled with a 6890 GC and 5973 Mass Selective Detector (Agilent Technologies). Micro-furnace program temperature: Initial T 50 °C; 20 °C min⁻¹ up to 200 °C; 8 °C min⁻¹ up to 500 °C; 20 °C min⁻¹ up to 700 °C. § Multi-Shot Pyrolyzer EGA/Py-3030D (Frontier Lab) coupled with a 6890 GC and 5973 Mass Selective Detector (Agilent Technologies). Pyrolysis T: 550 °C; HMDS for the *in situ* silylation of pyrolysis products.

2.1. Biskupin Archaeological Site (Poland)

Found in 1933, Biskupin was a fortified settlement dating to the Bronze Age (around mid-8th century BC). The site stretches across an area of about 2 ha. Between 1934 and 1974 several excavation campaigns were carried out [64,65], at the end of which the findings included a sizeable amount of oak and pine wood. An *in-situ* conservation strategy was adopted, based on keeping the wood remains in the environment where they were found,

ground or water. A complete description of the chemical analysis of wood samples from the Biskupin site is presented in [7].

2.2. “La Marmotta” Archaeological Site (Italy)

This Neolithic village (ca. 5500 BC) found in the Bracciano lake, near Rome (Italy), is now 8 m below the water level and is recognised as the most ancient Stone Age shore village in Western Europe. Since 1989, the archaeological excavations have resulted in the recovery of a variety of pottery, botanical, faunal, lithic, and wooden remains. In particular, 3000 wood piles were discovered in the mud of the lake, originally used to uphold the stilt houses of the village. The large number of piles suggests that the village was an important settlement [33,66,67].

The results discussed here refer to the analysis of samples collected at increasing depths from the surface of an oak pile. Detailed information can be found in [33,62].

2.3. The Oseberg Collection (Norway)

The Viking Ship Museum in Oslo (Norway) exhibits and preserves a significant part of Viking Age wooden objects discovered near Tønsberg, Oseberg burial mound (834 AD) [68]. The burial pertained to two women of high standing and contained the Oseberg ship, a variety of metal artefacts and textiles, and a number of unique wooden objects including a ceremonial wagon, sleds, and animal head posts, cooking equipment, weaving and agricultural tools [69]. Many of the artefacts were treated with alum salts in the early 1900s, soon after their discovery, and the presence of unstable salts derived from alum has caused dramatic conservation problems, which are threatening the preservation of the collection. The results of the Py(HMDS)-GC/MS analysis of the alum-treated wood samples are presented. A wider overview of the research can be found in [8,10,12,70].

2.4. The Ancient Harbour of San Rossore (Pisa, Italy)

The archaeological findings of San Rossore, uncovered in December 1998, are related to the urban harbour operating during the Etruscan and Roman periods in Pisa (Italy) [71]. During the excavations, the remains of 31 shipwrecks were found. The ships were covered by clay silt and sand, however, part of them were in a good condition. Wooden elements were waterlogged and presented a spongy consistency due to their permanence underwater, but the structures of the ships were well preserved. The archaeological artefacts from the site date to a period between the 2nd century BC and the 4th century AD. The description of the investigation carried out on wood materials from the site is presented in [31,54].

2.5. Żółte Archaeological Site (Poland)

The Żółte site is located on an island on lake Zarańskie, in the Drawsko region in Poland. Wooden remains pertaining to the settlement are dated from the end of the 11th to the beginning of the 12th century. They mainly include well-preserved structures along the shore, such as palisades and bridges [72,73]. The artefacts played both a functional and symbolic role in the context of religious/ritual ceremonies. The investigation carried out on wood materials from the Żółte site is presented in [37].

2.6. The Lyon Shipwrecks (France)

Sixteen wrecks were discovered during excavations of the Parc Saint-Georges in the Rhone region (France), situated on what was once the bank of the Saône River. The Lyon2 ship was a Gallo-Roman barge dated to the 2nd century AD. Sample Ly-A0 was from an untreated pine wood part, which was highly contaminated by iron salts, mainly pyrite. Sample Ly-A1 was from an oak wood part also contaminated by iron salts, treated with a solution of 20% PEG 4000 and 10% disodium sebacate, and freeze-dried [74]. The aim of the treatment was to consolidate the wood and to limit the effects of the acidification. More details about the samples and the results are presented in [36].

3. Results and Discussion

The following sections illustrate the results that can be obtained from each analytical pyrolysis-based technique discussed in this review, highlighting the insight that can be gained about lignin alteration. The results of some published case studies are presented and, in some cases, re-interpreted and compared, providing a holistic view of what can be achieved with these techniques.

3.1. Direct Exposure Mass Spectrometry (DE-MS)

The instrumental assets where pyrolysis products are directly identified by MS without chromatographic separation step are referred to as Pyrolysis Mass Spectrometry (Py-MS), Direct Exposure Mass Spectrometry (DE-MS) or Direct Temperature resolved Mass Spectrometry (DT-MS). Apart from some differences in the instrumental apparatus, the three analytical techniques are based on the same principle: The sample is desorbed or pyrolysed by controlled heating directly into the ion source [46,50–52,54,75–80]. Pyrolysis coupled directly to mass spectrometry allows for reduction of analysis time and extends the detectability of pyrolysis fragments to structures too large for gas chromatography analysis. At the same time, the results are generally difficult to interpret, as an overall mass spectrum of all pyrolysis products is obtained. For this reason, multivariate analysis of mass spectral data, such as principal component analysis (PCA), has sometimes been used to compare, differentiate, and classify the samples [38,48–52,54].

DE-MS and PCA were applied to study the state of degradation of archaeological waterlogged wood and, in particular, investigate the chemical modification of lignin fraction in the objects from two Italian archaeological sites (the Ancient Harbour of Pisa San Rossore [54] and La Marmotta [33]) and from the two Polish archaeological sites (Biskupin and Żółte [39,53]). The results were compared to those obtained for sound non-degraded wood of the same species, such as pine (*Pinus pinaster*), oak (*Quercus robur*), elm (*Ulmus minor*), alder (*Alnus glutinosa*), and beech (*Fagus sylvatica*).

Analysis of DE-MS mass spectral data corresponding to the mass range 50–350 m/z was performed by principal component analysis (PCA, Nipals algorithm) [81] on the covariance matrix of centred data, after row normalisation of the full 50–500 m/z spectra. The region 50–350 m/z was selected because it contains all the pyrolysis fragments corresponding to lignin monomers and dimers. The software used was XLSTAT 2009.1.02. (Addinsoft, Paris, France).

Figure 1 shows the mass spectra obtained by the analysis of a reference oak wood sample, one sample from the outermost part of a pile from La Marmotta, and one sample from fragment 6 (oak wood) collected from the Biskupin site. The mass spectra showed high complexity. The results were interpreted on the basis of the attribution of m/z values [33]. Table 2 lists the fragments identified and the most probable assignments, based on the mass spectra of guaiacyl and syringyl compounds produced in the pyrolysis of lignin.

Table 2. Molecular assignment of the most abundant m/z values observed in the DE-MS mass spectra of lignin. L—lignin; C—carbohydrates; G—guaiacyl-lignin; S—syringyl-lignin.

m/z	Molecular Origin	Wood Component	References
65	present in many pyrolysis products of both lignin and carbohydrates	L/C	[82–84]
77	present in many pyrolysis products of both lignin and carbohydrates	L/C	[82–84]
91	alkylbenzenes	L	[83]
94	phenol	L	[52,82–84]

Table 2. Cont.

<i>m/z</i>	Molecular Origin	Wood Component	References
107	alkylphenols	L	[52,83]
110	1,2-dihydroxybenzene; 1,4-dihydroxybenzene; 5-methyl-2-furaldehyde; 2-acetylfuran	L/C	[54,82–84]
123	4-methylcatechol; 4-methylguaiacol; dihydrocaffeic acid	L	[52,54,83,84]
124	guaiacol; 4-methylcatechol; coniferyl alcohol	G	[38,52,54,83,84]
137	4-ethylguaiacol; 4-propylguaiacol; coniferyl alcohol; dihydroconiferyl alcohol; guaiacylacetone, homovanillin	G	[38,52,54,83,84]
138	4-methylguaiacol	G	[38,52,54,83,84]
150	4-vinylguaiacol	G	[38,52,54,83,84]
151	vanillin; acetovanillone; vanillic acid methyl ester; propiovanillone; guaiacyl vinyl ketone; vanillic acid	G	[38,52,54,83,84]
152	4-ethylguaiacol; vanillin; coniferyl alcohol	G	[38,52,54,83,84]
154	Syringol	S	[38,52,54,83,84]
164	eugenol; isoeugenol (E and Z); p-coumaric acid	G	[38,52,54,83,84]
166	acetovanillone; 4-propylguaiacol	G	[52,54,83,84]
167	4-ethylsyringol; 4-propylsyringol; sinapyl alcohol; dihydrosinapyl alcohol; syringylacetone	S	[38,52,54,83,84]
168	vanillic acid; 4-methylsyringol	G/S	[38,52,54,83,84]
178	Coniferylaldehyde	G	[38,52,54,83,84]
180	coniferyl alcohol, 4-vinylsyringol; guaiacylacetone; propiovanillone	G/S	[38,52,54,83,84]
181	syringaldehyde; acetosyringone; syringic acid methyl ester; propiosyringone; syringyl vinyl ketone; syringic acid	S	[38,52,54,83,84]
182	4-ethylsyringol; syringaldehyde; dihydroconiferyl alcohol; vanillic acid methyl ester; dihydrocaffeic acid; sinapyl alcohol	S/G	[52,54,83,84]
194	4-(1-propenyl)syringol, 4-(2-propenyl)syringol (E and Z); 4-allylsyringol; ferulic acid	S	[38,52,54,83,84]
196	acetosyringone; 4-propylsyringol	S	[38,52,54,83,84]
198	Syringic acid	S	[38,52,54,83,84]
208	Sinapylaldehyde	S	[38,52,54,83,84]
210	sinapyl alcohol; syringylacetone; propiosyringone	S	[38,52,54,83,84]
212	dihydrosinapyl alcohol; syringic acid methyl ester	S	[52,54,83,84]
272	stilbene-type dimer	G-G dimer	[38,52]
302	stilbene-type dimer	G-S dimer	[38,52]
332	stilbene-type dimer	S-S dimer	[38,52]
358	β -resinol type dimer	G-G dimer	[38,52]
388	β -resinol type dimer	G-S dimer	[38,52]
418	β -resinol type dimer	S-S dimer	[38,52]

The archaeological samples, as expected, showed low signals of carbohydrates compared to the reference sample [54]. The sample from Biskupin still contained some carbohydrates, as highlighted by the intensity of the peaks at *m/z* 65 and 77 [52], whereas the sample from La Marmotta was mainly composed of lignin (Figure 1).

In addition to the possibility of evaluating the state of degradation of wood from the polysaccharide point of view, it is also possible to observe some degradation processes occurring in the lignin fraction following some characteristic *m/z* values.

The peaks at m/z 137 and m/z 167 are commonly present in the mass spectra of sound wood and are generated by the fragmentation of *p*-substituted guaiacyl or syringyl compounds, respectively. The first one corresponds to the 4-methylguaiacol ion and is present in the mass spectra of 4-ethylguaiacol, 4-propylguaiacol, coniferyl alcohol, and dihydroconiferyl alcohol. The latter corresponds to the 4-methylsyringol ion and is present in syringyl derivatives, listed in Table 2.

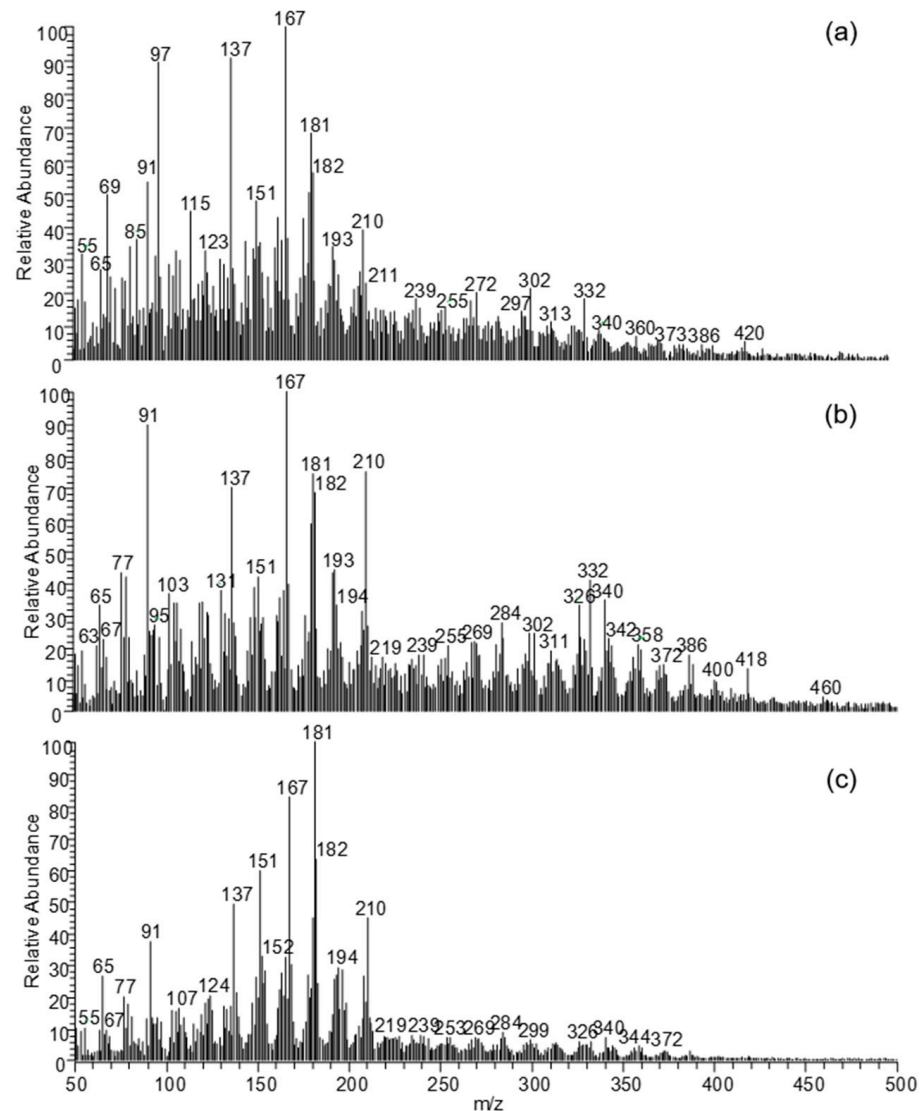


Figure 1. DE-MS mass spectra of a reference sound oak sample (a), samples of archaeological oak wood from Oak 6 from Biskupin site (b) and La Marmotta (2212-B) (c).

The oxidation processes occurring in the lignin fraction of archaeological wood can be monitored through the characteristic fragments formed by compounds with carbonyl or carboxyl functionalities such as m/z 151 from guaiacyl units and m/z 181 from syringyl ones. In particular, the fragment with m/z 151 is due to the 4-(1-oxomethyl)-guaiacol ion, whereas m/z 181 corresponds to the ion with an additional methoxyl functionality, the 4-(1-oxomethyl)-syringol ion. In fact, the former can be generated by the fragmentation of vanillin, acetovanillone, propenylguaiacol, guaiacyl vinyl ketone, vanillic acid, and vanillic acid methyl ester, whereas the latter is formed during the fragmentation of syringaldehyde, acetosyringone, propiosyringone, syringyl vinyl ketone, syringic acid, and syringic acid methyl ester.

By comparing the fragments deriving from the oxidised lignin products with those at m/z 137 and 167, it is possible to have an estimation of the oxidation level of this polymer. In fact, the increase in the relative abundance of the peaks at m/z 151 and 181 with respect to the peaks at m/z 137 and 167 was evident in the archaeological samples compared to the reference, and in particular for La Marmotta sample, indicating an increase in lignin oxidation [33].

The level of lignin depolymerisation is another index of its degradation. The peaks related to the lignin polymerisation state are those at m/z 272, 302, and 332, which correspond to dimers (Table 2). In fact, these fragments were negligible in the mass spectra obtained from La Marmotta sample (Figure 1c), indicating that lignin degradation reactions involved partial depolymerisation, resulting in the cleavage of these dimeric bonds. On the other hand, in the Biskupin samples, dimer fragments were evident in the mass spectra, highlighting a better preservation of lignin. In fact, the presence and relative intensity of the lignin dimer fragments in the pyrolysis mass spectral profiles can be used as a probe to estimate lignin depolymerisation, but they can also give information on the state of lignin-carbohydrate bonds. The fact that dimer fragments were more evident in the Biskupin sample than in the sound wood sample can be interpreted as an indication of degraded polysaccharides, which make lignin more prone to undergo extensive pyrolytic degradation.

Despite the qualitative information that can be directly obtained from observing the MS spectra, DE-MS analysis is generally used to obtain a high number of spectra, which still contain much information hidden underneath complex data. PCA is therefore used as an effective pattern recognition tool in order to compare the results and highlight differences and similarities among the samples and correlation between variables.

Figure 2 shows the score plot obtained for the first two principal components (PCs), which accounted for ca. 74% of the total variance. It is evident that PC1 is correlated to the intensities of the peaks generated from the syringyl units (positive values of the PC1) and correlated negatively to the guaiacyl ones (m/z 124, 137). Since the pine wood samples do not contain syringyl-lignin, they are placed in the negative range of PC1. Therefore, PC1 discriminating between softwoods and hardwoods gives a rapid indication of the type of wood and of the ratio between the amounts of syringyl and guaiacyl fragments. Due to the difference in lignin composition, softwood samples are located at low values of PC1, whereas hardwood samples are located at higher values of PC1.

PC2 in the range of positive values is correlated to the fragments produced during the fragmentation of the polysaccharide fraction (m/z 55, 69, 73, 85, 97, 114, 126) [54]. This main component differentiates samples on the basis of holocellulose content and can provide an indication of wood degradation. All the waterlogged archaeological samples are positioned at the bottom of the PC2/PC1 score plot. This indicates their lower polysaccharide content when compared to reference samples of the same species. The significance of comparing the results obtained from archaeological wood with reference wood of the same species is particularly highlighted by Figure 2, in which one of the oak archaeological samples from Biskupin (PC1score: -0.168 , PC2score: 1.509) almost overlaps with the beech reference wood (PC1score: -0.161 , PC2score: 1.432). This sample would have been considered in a very good state of preservation, if compared to the wrong type of hardwood. Oak wood is known to be particularly rich in polysaccharides compared to beech wood. The archaeological oak wood, despite being degraded, preserves the polysaccharides at the level of fresh, non-degraded birch wood.

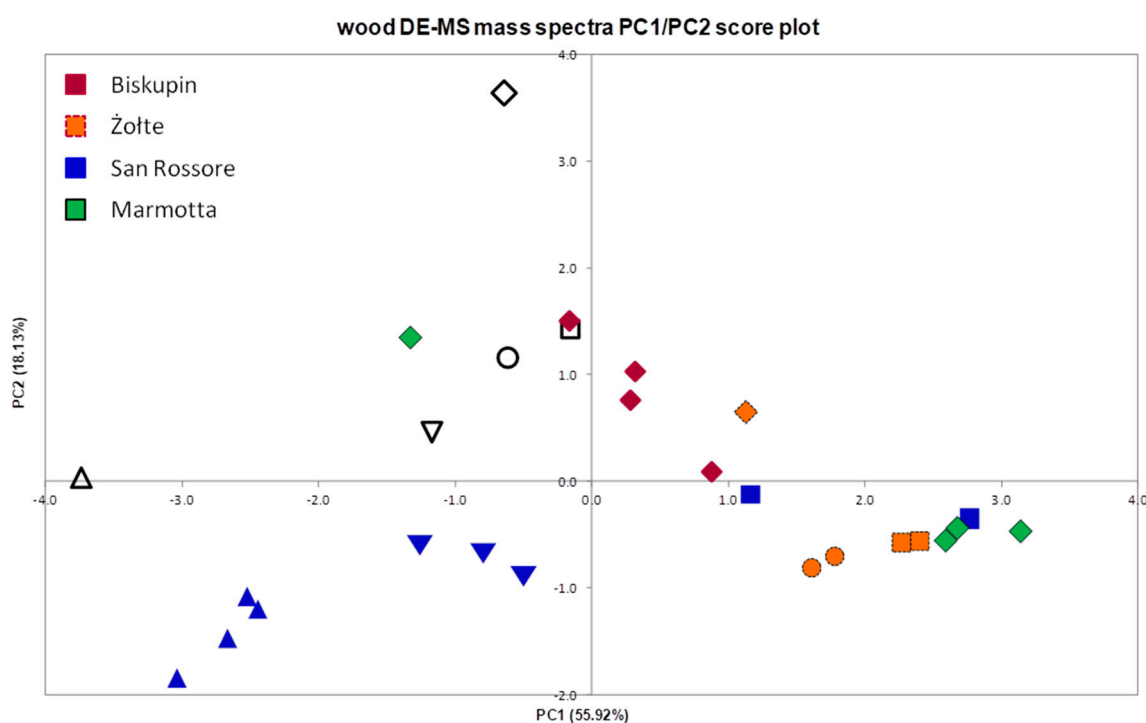


Figure 2. PCA (principal component analysis) score plot of the DE-MS mass spectral data obtained from reference and archaeological wood samples collected from the four archaeological sites in Italy and Poland. Sound wood: \diamond -oak, \square -beech, \circ -alder, ∇ -elm, \triangle -pine; Archaeological wood: \blacklozenge -oak, \blacksquare -beech, \bullet -alder, \blacktriangledown -elm, \blacktriangle -pine.

3.2. Evolved Gas Analysis Mass Spectrometry (EGA-MS)

In EGA-MS, pyrolysis is also directly coupled to mass spectrometry. However, a temperature program is used instead of a single pyrolysis shot at fixed temperature, thus the products generated during heating are transferred to the mass spectrometer as a function of time (and pyrolysis temperature) at which they are produced. The result is the so-called total ion thermogram (TIT). The mass spectra obtained at different temperatures are overall mass spectra, as in the case of DE-MS, but the slow heating enables more detailed information to be obtained on the thermal degradation features of the sample components. In addition, single ions can be isolated, and their evolution profile extracted (extracted ion thermogram—EIT), thus providing a more selective chemical information. The results obtained by applying EGA-MS to the archaeological wood samples from La Marmotta are discussed in Tamburini et al. [33].

Figure 3 shows the total ion thermograms (TITs) of a series of archaeological wood samples collected at increasing depths from the surface of pile 2212, where A corresponds to the surface and G to the core of the pile [33]. A comparison with the sound oak reference wood is provided and the mass spectra relative to the main regions of thermal degradation are reported. The sound oak wood undergoes thermal degradation in three stages, in agreement with multiple studies [33,36]. The thermal degradation of all the wood components (hemicelluloses, cellulose, and lignin) begins below 300 °C, as suggested by the presence of peaks assigned to both carbohydrates (m/z 60, 85, 96, 114) and lignin (m/z 137, 167, 180, 194, 208) (Table 2). The most abundant peak in the mass spectrum (Figure 3a) is m/z 114, representative of hemicelluloses [85,86]. The second zone, between 300 and 400 °C, corresponds to the main thermal degradation of cellulose, as showed by the most abundant peak at m/z 60, which derives from the mass fragmentation of levoglucosan [33,82–84]. The third zone above 400 °C corresponds to the formation of phenol and catechol structures (m/z 108, 110 and 123) [33,82–84], which are secondary

lignin pyrolysis products [87,88]. Lignin dimers (m/z 272, 302 and 332) are also produced at high temperature [33,52].

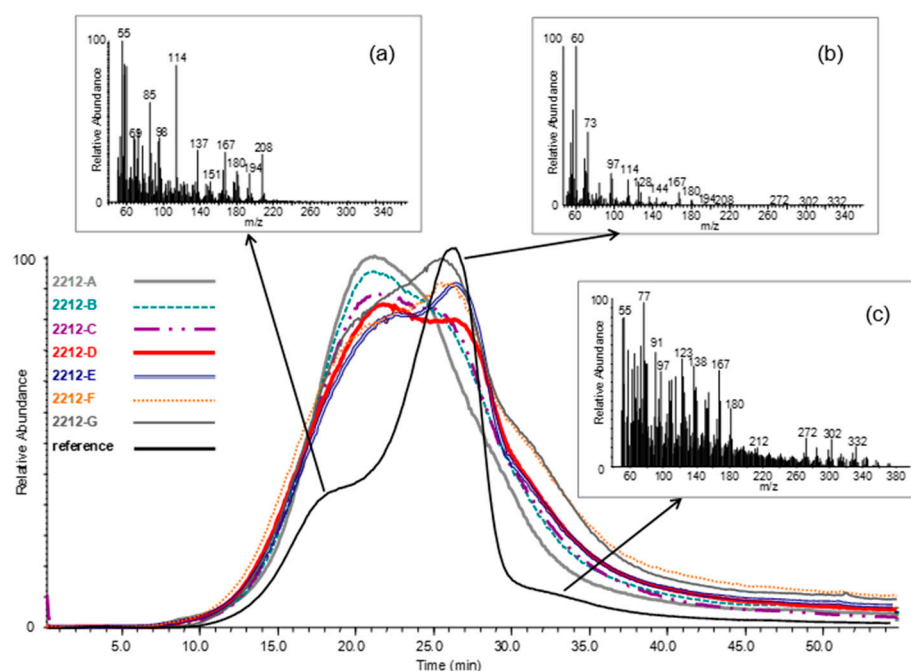


Figure 3. Total ion thermograms (TITs) of sound oak wood (reference) and archaeological wood samples from pile 2212 from “La Marmotta” collected at increasing depths from the surface (A—surface, G—core) and mass spectra extracted from the three thermal degradation regions of sound oak wood. (a) Below 300 °C, (b) between 300 °C and 400 °C, and (c) above 450 °C.

Archaeological wood samples underwent thermal degradation approximately in the same temperature range observed for the reference sample, but they showed very different profiles. A progressive shift of the maximum degradation temperature towards a lower temperature was observed when proceeding from the core to the surface of the pile, indicating that less thermal energy was necessary to thermally degrade the lignocellulosic material. The reduced thermal stability can be explained by a more degraded wood structure. The detailed shoulders present in the profile of sound wood were no longer observed in the TITs of the archaeological wood samples, as a result of cellulose loss [33]. The mass spectra finally revealed that lignin was the main component present in the outermost part of the pile [33]. Lignin dimers were only detected in the innermost samples 2212-D, E, F, and G (Figure 4).

Extracted ion thermograms (EITs) enabled the evolution of specific ions to be followed, therefore the thermal range of formation of specific pyrolysis products was determined. In addition, the area of the EITs can be integrated, thus enabling semi-quantitative calculations to be performed. This represents another powerful way to highlighting differences among samples. Figure 5 shows the EITs (m/z 107, 123, 167, 181 and 272, Table 2) for sample 2212-B (close to the surface of the pile) and for sample 2212-F (close to the core).

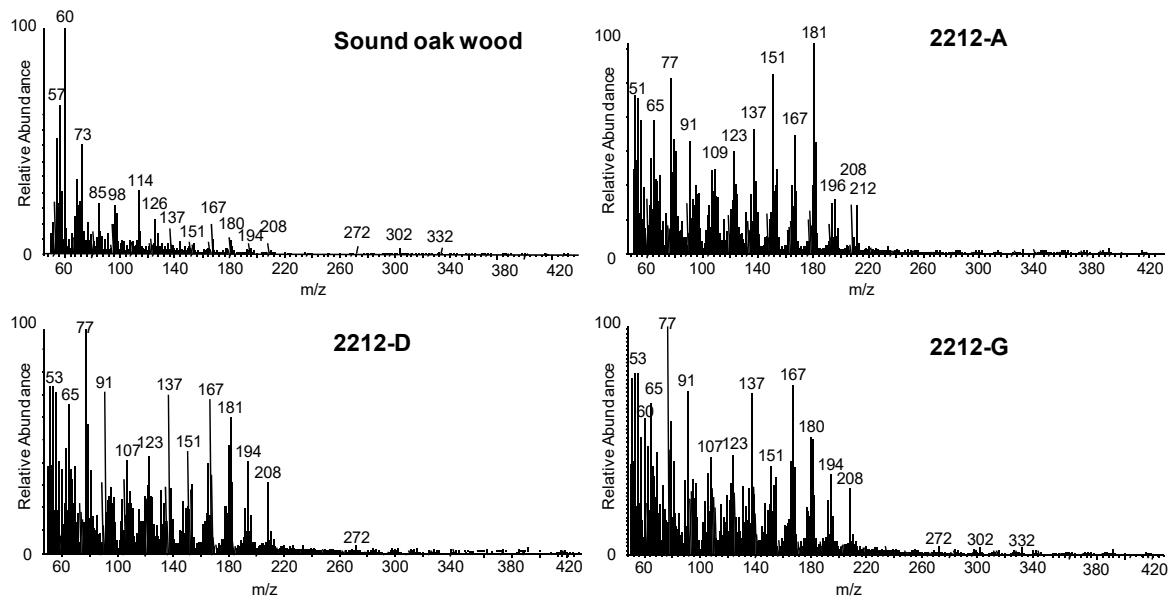


Figure 4. Overall mass spectra obtained by EGA-MS analysis of sound oak wood and archaeological wood samples collected at different depths from the surface, in the surface (A—rings 11–15), in the middle (D—rings 26–30), and in the core (G—rings 46–48) of pile 2212 from La Marmotta. Adopted from [33].

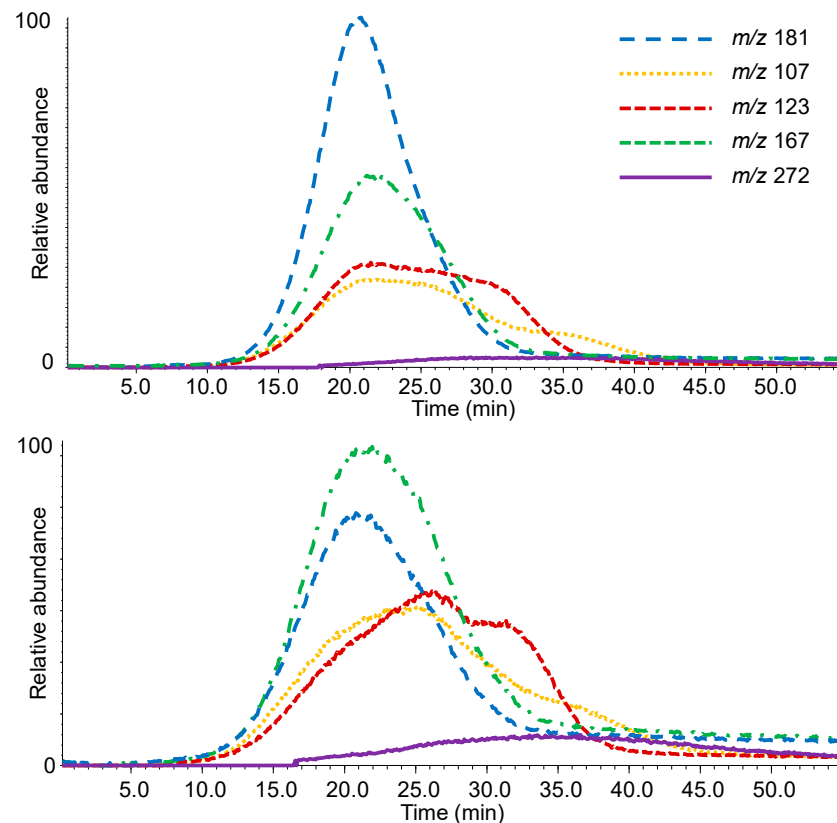


Figure 5. Extracted ion thermograms (EITs) of specific m/z values for sample B (rings 16–20) from the surface (**top**) and sample F (rings 41–45) from the core (**bottom**) of pile 2212 from La Marmotta.

The lignin alteration in the archaeological woods was also evaluated considering the peaks at m/z 151 and 181, characteristic of the lignin oxidation, at m/z 272, 302, and 332,

related to the level of lignin depolymerisation, and at m/z 137 and 167, indicative of guaiacol and syringol species *p*-substituted with a free benzylic position (Table 2).

In order to evaluate the level of lignin oxidation, the ratios between the areas of specific m/z EITs were calculated. The oxidation level of guaiacyl (G index) and syringyl (S index) lignin was calculated from the Equations (1) and (2).

$$\text{S index} = \text{EITs } m/z \text{ 181} / (\text{EITs } m/z \text{ 181} + \text{EITs } m/z \text{ 167}) \quad (1)$$

$$\text{G index} = \text{EITs } m/z \text{ 151} / (\text{EITs } m/z \text{ 151} + \text{EITs } m/z \text{ 137}) \quad (2)$$

Lignin depolymerisation level was evaluated on the basis of the yield of dimer formation of dimers during heating. D index was calculated from the Equation (3).

$$\text{D index} = \text{EITs } m/z \text{ (272 + 302 + 332)} / \text{EITs } m/z \text{ (151 + 181 + 137 + 167 + 272 + 302 + 332)} \quad (3)$$

The results of these calculations are shown in Figure 6, where the trends in oxidation and depolymerisation at different depths from the surface of pile 2212 is clearly highlighted.

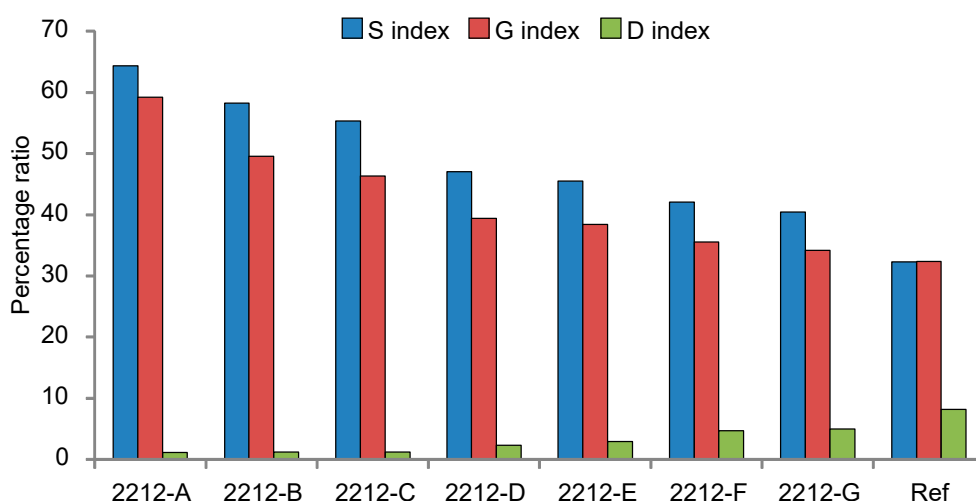


Figure 6. Percentage ratios indicative of syringyl lignin oxidation (S index), guaiacyl lignin oxidation (G index), and formation of dimers (D index) in EGA-MS analysis of the wood pile 2212 from La Marmotta site at different depths from the surface, where A—surface, G—core, Ref—reference, (sound non-degraded oak wood sample).

G index and S index increased from the core to the surface of the pile, proving a gradual increase in lignin oxidation. The S index of sample A was slightly higher than the G index, which also confirmed that syringyl-lignin is more prone to oxidation than guaiacyl lignin [25,89–91]. On the other hand, the D index increased from the outside to the inside of the pile. Reference wood featured the highest D index, indicating that a significant number of lignin dimers are produced in the pyrolysis conditions adopted. The general decrease in the formation of dimers during the pyrolysis of archaeological wood was therefore related to an increasing depolymerisation of lignin moving to the external parts of the pile.

3.3. Single-Shot Py(HMDS)-GC/MS

In this section, the ability of Py-GC/MS with in situ silylation to estimate wood preservation is discussed by presenting several case studies.

The main advantage of Py-GC/MS over techniques that are directly coupled with mass spectrometry is the selectivity in the identification of pyrolysis products, thanks to a chromatographic separation step before MS analysis. This enables the abundance of specific pyrolysis products to be related to different degradation patterns. Figure 7 shows the chromatographic profiles obtained by Py(HMDS)-GC/MS of sound and archaeological wood samples from Biskupin, La Marmotta, and the Oseberg collection. Table 3 shows the

identification of trimethylsilyl derivatives of wood pyrolysis products, which can also be found in recent publications [7,8,62,92]. The wood pyrolysis products were attributed to holocellulose (H) and lignin (L). In addition, guaiacyl- (G) and syringyl-lignin (S) can be easily distinguished (Table 3). From a qualitative point of view, all archaeological samples showed different profiles, indicating different preservation states of the wood components. A relatively simpler chromatographic profile, showing mainly lignin pyrolysis products with a very low abundance of pyrolysis products deriving from holocellulose, was obtained for the Oseberg sample (Figure 7d). Vanillic (#85) and syringic (#95) acids were the most abundant peaks in the chromatogram.

Table 3. List of wood pyrolysis products identified by Py(HMDS)-GC/MS. In the case of lignin pyrolysis products, lignin categories (L. cat.) are indicated: SC—short chain; LC—long chain; M—monomers; C—carbonyl; A—acids; D—demethylated/demethoxylated; E—esters; and O—others. The other pyrolysis products mainly derive from holocellulose.

N°	Compound	L. cat.	N°	Compound	L. cat.
1	1,2-dihydroxyethane (2TMS)		59	5-methyl-3-methoxy-1,2-benzenediol (2TMS)	D
2	2-hydroxymethylfuran (TMS)		60	4-ethylsyringol (TMS)	SC
3	phenol (TMS)		61	<i>E</i> -isoeugenol (TMS)	LC
4	2-hydroxypropanoic acid (2TMS)		62	1,4-anhydro-D-galactopyranose (2TMS)	
5	2-hydroxyacetic acid (2TMS)		63	1,6-anhydro-D-galactopyranose (2TMS)	
6	1-hydroxy-1-cyclopenten-3-one (TMS)		64	2-hydroxymethyl-5-hydroxy-2,3-dihydro-(4H)-pyran-4-one (2TMS)	
7	3-hydroxymethylfuran (TMS)		65	4-vinylsyringol (TMS)	SC
8	<i>o</i> -cresol (TMS)		66	1,4-anhydro-D-glucopyranose (2TMS at position 2,4)	
9	2-furancarboxylic acid (TMS)		67	1,2,4-trihydroxybenzene (3TMS)	
10	unknown holocellulose I		68	acetovanillone (TMS)	C
11	<i>m</i> -cresol (TMS)		69	4-hydroxybenzoic acid (2TMS)	A
12	2-hydroxy-1-cyclopenten-3-one (TMS)		70	4-propenylsyringol (TMS)	LC
13	<i>p</i> -cresol (TMS)		71	1,6-anhydro- β -D-glucopyranose (2TMS at position 2,4)	
14	3-hydroxy-(2H)-pyran-2-one (TMS)		72	vanillic acid methyl ester (TMS)	E
15	unknown holocellulose II		73	5-vinyl-3-methoxy-1,2-benzenediol (2TMS)	D
16	unknown holocellulose III		74	<i>Z</i> -4-isopropenylsyringol	LC
17	<i>Z</i> -2,3-dihydroxycyclopent-2-enone (TMS)		75	1,4-anhydro-D-galactopyranose (3TMS)	
18	<i>E</i> -2,3-dihydroxycyclopent-2-enone (TMS)		76	unknown lignin I	O
19	1,2-dihydroxybenzene (TMS)		77	syringaldehyde (TMS)	C
20	3-hydroxy-(4H)-pyran-4-one (TMS)		78	2,3,5-trihydroxy-4H-pyran-4-one (3TMS)	
21	5-hydroxy-(2H)-pyran-4(3H)-one (TMS)		79	1,6-anhydro- β -D-glucopyranose (3TMS)	
22	2-hydroxymethyl-3-methyl-2-cyclopentenone (TMS)		80	1,4-anhydro-D-glucopyranose (3TMS)	
23	1-hydroxy-2-methyl-1-cyclopenten-3-one (TMS)		81	<i>E</i> -4-isopropenylsyringol (TMS)	LC
24	1-methyl-2-hydroxy-1-cyclopenten-3-one (TMS)		82	1,6-anhydro- β -D-glucofuranose (3TMS)	

Table 3. Cont.

N°	Compound	L. cat.	N°	Compound	L. cat.
25	1,3-dihydroxyacetone (2TMS)		83	unknown lignin II	O
26	guaiacol (TMS)	SC	84	unknown lignin III	O
27	unknown holocellulose IV		85	vanillic acid (2TMS)	A
28	3-hydroxy-6-methyl-(2H)-pyran-2-one (TMS)		86	acetosyringone (TMS)	C
29	unknown holocellulose V		87	5-propyl-3-methoxy-1,2-benzenediol (2TMS)	D
30	2-methyl-3-hydroxy-(4H)-pyran-4-one (TMS)		88	coumaryl alcohol (2TMS)	D
31	2-methyl-3-hydroxymethyl-2-cyclopentenone (TMS)		89	syringic acid methyl ester (TMS)	E
32	2,3-dihydrofuran-2,3-diol (2TMS)		90	vanillylpropanol (2TMS)	LC
33	2-furylhydroxymethylketone (TMS)		91	Z-coniferyl alcohol (2TMS)	M
34	5-hydroxymethyl-2-furaldehyde (TMS)		92	4-hydroxy-3,5-dimethoxycinnamic acid methyl ester (TMS)	E
35	4-methylguaiacol (TMS)	SC	93	coniferylaldehyde (TMS)	C
36	1,2-dihydroxybenzene (2TMS)		94	trihydroxycinnamyl alcohol (3TMS)	D
37	2-hydroxymethyl-2,3-dihydropyran-4-one (TMS)		95	syringic acid (2TMS)	A
38	1,4:3,6-dianhydro- α -D-glucopyranose (TMS)		96	unknown lignin IV	O
39	Z-2,3-dihydroxycyclopent-2-enone (2TMS)		97	E-coniferyl alcohol(2TMS)	M
40	4-methylcatechol (2TMS)	D	98	3,4-dihydroxy-5-methoxybenzoic acid (3TMS)	A
41	4-ethylguaiacol (TMS)	SC	99	syringylpropanol (2TMS)	LC
42	syringol (TMS)	SC	100	Z-sinapyl alcohol (2TMS)	M
43	1,4-dihydroxybenzene (2TMS)		101	unknown lignin V	O
44	arabinofuranose (4TMS)		102	3,4-dihydroxycinnamyl alcohol (3TMS)	D
45	4-vinylguaiacol (TMS)	SC	103	trihydroxycinnamyl alcohol I (3TMS)	D
46	3-hydroxy-2-hydroxymethyl-2-cyclopentenone (2TMS)		104	sinapylaldehyde (TMS)	C
47	E-2,3-dihydroxycyclopent-2-enone (2TMS)		105	trihydroxycinnamyl alcohol II (3TMS)	D
48	4-ethylcatechol (2TMS)	D	106	Z-2-methoxy-3,4-dihydroxycinnamyl alcohol (3TMS)	D
49	3-hydroxy-2-(hydroxymethyl)cyclopenta-2,4-dienone (2TMS)		107	sinapyl alcohol (TMS)	M
50	eugenol (TMS)	LC	108	E-sinapyl alcohol (2TMS)	M
51	4-methylsyringol (TMS)	SC	109	E-2-methoxy-3,4-dihydroxycinnamyl alcohol (3TMS)	D
52	3-methoxy-1,2-benzenediol (2TMS)	D	110	unknown lignin VI	O
53	3,5-dihydroxy-2-methyl-(4H)-pyran-4-one (2TMS)		111	unknown anhydrosugar I (dimer)	
54	1,6-anhydro- β -D-glucopyranose (TMS at position 4)		112	unknown anhydrosugar II (dimer)	

Table 3. Cont.

N°	Compound	L. cat.	N°	Compound	L. cat.
55	1,6-anhydro- β -D-glucopyranose (TMS at position 2)		113	unknown anhydrosugar III (dimer)	
56	Z-isoeugenol (TMS)	LC	114	unknown anhydrosugar IV (dimer)	
57	vanillin (TMS)	C	115	unknown anhydrosugar V (dimer)	
58	1,2,3-trihydroxybenzene (3TMS)		116	unknown anhydrosugar VI (dimer)	

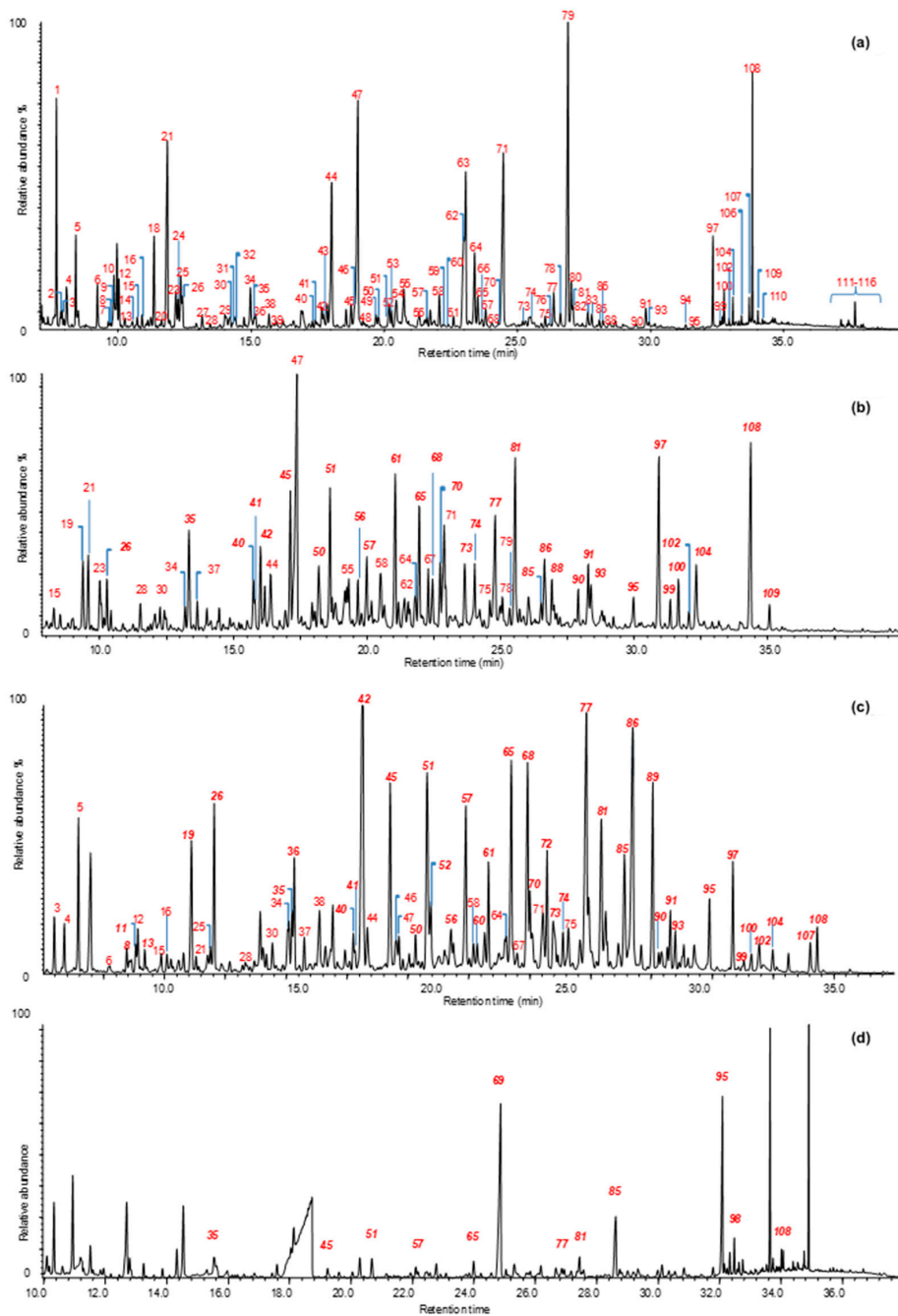


Figure 7. Py(HMDS)-GC/MS chromatographic profiles of (a) sound oak wood sample, (b) sample 4A from Biskupin [7], (c) sample 2212-A from La Marmotta, and (d) sample 185-6 from the Oseberg collection [8]. Peak labelling refers to Table 3. In *Italics*: Lignin pyrolysis products.

The parameter usually considered when evaluating the chemical degradation of wood is the holocellulose/lignin (H/L) ratio [15]. Generally, with regards to archaeological wood, this index provides information on the preferential loss of one wood component (mainly holocellulose) by comparing the values obtained for degraded and sound wood of the same species. Table 4 shows the H/L ratios obtained by Py-GC/MS analysis of selected samples from Biskupin [7], La Marmotta [62], Oseberg [8], and reference sound wood samples, such as oak wood for the samples from Biskupin and La Marmotta, and birch wood for the Oseberg samples.

The data obtained analysing wood from La Marmotta and the Oseberg collection could apparently suggest that all the samples have similar states of preservation, since they had all undergone a substantial loss of polysaccharides. The results obtained for the Biskupin samples, on the other hand, showed a decreasing trend in preservation from the innermost sample (4C) to the outermost sample (4A). The Oseberg samples 185-1 and 185-6 showed very low H/L ratio, indicative of an almost complete absence of polysaccharide components, especially for sample 185-6. Nevertheless, it is evident that the H/L ratio does not provide information on the chemical changes occurring in the single wood components, nor on the state of preservation of the residual wood materials.

Table 4. Holocellulose (H) and lignin (L) content expressed as percentage values based on chromatographic areas; H/L ratios and syringyl/guaiacyl (S/G) ratios of reference and archaeological wood samples.

	Oak Ref	Biskupin			La Marmotta			Birch Ref	Oseberg	
		4A	4B	4C	2212A	2212D	2212G		185-1	185-6
Sum H (%)	77.1	38.0	63.8	74.4	14.4	14.4	21.1	75.6	20.3	3.2
Sum L (%)	22.9	62.0	36.2	25.6	85.6	85.6	78.9	24.4	79.7	96.8
H/L	3.4	0.6	1.8	2.9	0.2	0.2	0.3	3.1	0.3	0.0
S/G	1.6	1.1	1.7	2.3	1.3	1.9	2.3	2.4	1.4	1.7

A useful parameter in the evaluation of the preservation level of hardwood lignin by Py-GC/MS is the syringyl/guaiacyl (S/G) ratio, which is related to alterations of methoxy groups in lignin [93].

The S/G ratios of the analysed samples are reported in Table 4. The reference samples showed, as expected, very different values: 1.3 for oak wood and 2.4 for birch wood, indicating that the two species have a different distribution of guaiacyl and syringyl components in the lignin network. The interpretation of the results obtained for archaeological samples is not straightforward. The most common scenario is to obtain a lower S/G ratio for degraded samples, as the syringyl component of lignin is less resistant to chemical changes than the guaiacyl component, due to the presence in the syringyl lignin of additional methoxy groups on the aromatic ring that can be partially cleaved [90,91]. This was observed in the Oseberg samples, but not in all the samples from the other archaeological sites. However, S/G value may also be affected by several factors. For example, if both syringyl and guaiacyl units undergo demethylation/demethoxylation, the phenomenon is not highlighted by the S/G ratio. Consequently, although a change in the S/G ratio may be a first indication that the lignin has also undergone chemical changes, a more detailed data analysis is often needed.

In order to highlight the chemical modification undergone by the residual lignin, a strategy based on the categorisation of lignin pyrolysis products strategy can be adopted. The pyrolysis products generated from the lignin are classified according to their molecular structure and pyrolytic formation [7,8,62]. The sum of the peak areas of the pyrolysis products assigned to each category (L. cat., Table 3) is expressed as a percentage of the total relative abundance of all lignin pyrolysis products. In sound wood, the lignin pyrolysis products are usually distributed in a similar way, irrespective of the wood species [7]. Monomeric structures (coniferyl and sinapyl alcohols) account for the 40–50% of the total. The rest are composed of guaiacyl and syringyl units *p*-substituted by “short” (up to 2 carbon atoms) and “long” (3 carbon atoms) alkyl chains (about 20%), carbonyl

compounds (10–15%), and demethylated/demethoxylated compounds (15–20%). A very small abundance of pyrolysis products bearing an acidic functionality is usually present in the pyrolysis profiles of sound wood (3–5%).

The characterisation of archaeological wood samples led to totally different data (Figure 8). The relative abundance of “monomers” was usually lower than that obtained for sound wood. On the other hand, an increase in “short chain compounds” was detected. The formation of the side chain compounds is connected to depolymerisation of lignin during the burial period [94] or to the higher yield of secondary pyrolytic reactions for aged wood compared to sound wood [7,87,88]. In both cases, the increase in the relative abundance of short side-chain phenols and the decrease in the relative abundance of monomeric structures can be taken as an indication that alterations in the side chain of the phenylpropane units of lignin have occurred during degradation. Long side-chain lignin pyrolysis products, which are defunctionalised monomers, also appeared with a higher relative abundance in samples from the Biskupin site and samples taken from the inner part of the pile from La Marmotta than in sound wood. The oxidation of lignin was highlighted by an increase in carbonyl and carboxyl functionalities [23,27,30], but the extent of oxidation observed in the Oseberg samples is exceptional even for very degraded archaeological wood [8].

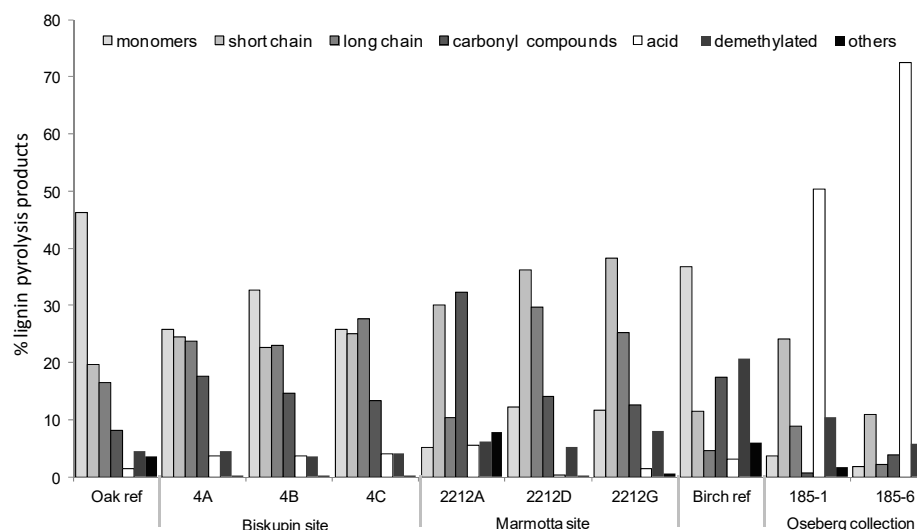


Figure 8. Abundances of the categories of lignin pyrolysis products expressed as percentages in the archaeological and the reference wood samples. The relative standard deviation obtained by Py-GC/MS of lignocellulosic materials is about 7%, as reported in the literature [7,30].

In terms of the detailed information that can be provided by Py(HMDS)-GC/MS, specific degradation products can be identified and related to specific degradation pathways. *p*-hydroxybenzoic acid (#69) was identified in all pyrograms obtained from the Oseberg samples. This pyrolysis product has not been previously reported as a lignin break-down product in naturally-aged archaeological samples [30–32,37,95]. The presence of this acid can be related to the oxidising conditions used in industrial processes to separate lignin from holocellulose, such as acidolysis and hydrolysis [96–100]. Thus, the results obtained for the Oseberg collection samples suggest that the alum treatment induced extreme oxidising conditions for lignin in the long term. The generation of *p*-hydroxybenzoic acid can be due to several reactions, including β -O-4' cleavage, demethoxylation, and side chain cleavage accompanied by extensive oxidation of lignin units. This was a robust proof of the role of the alum treatment in the dramatic degradation of these archaeological objects. In addition, the percentage abundance of acid lignin pyrolysis products was found to correlate with the concentrations of inorganic elements (Al, Fe, Ca) present in these samples [8].

As regards La Marmotta samples, the identification of methyl esters of vanillic (#72) and syringic acids (#89) with significantly high relative abundances allowed us to hypothesise a heat treatment as explanation for this particular lignin alteration. Heating wood to around 200–300 °C causes the formation of small molecules, including methanol [101,102], which can easily react in a gaseous phase with acidic moieties (vanillic and syringic acids), leading to the formation of methyl esters. The formation of methyl derivatives has also been observed during the heating of other materials as well, such as diterpenoid resins to produce pitch or tar from resinous woods [50]. Furthermore, the methyl derivatives of vanillic and syringic acids are known toasting markers of wooden barricades used in the production of wine [103–105]. Wood is also an insulating material, and when it is exposed to high temperatures, the surface can reach temperatures up to several hundred degrees, whereas the core (2–3 cm under the surface) remains at room temperature, thus explaining why these phenomena mainly involve the wood surface. The occurrence of methyl esters of vanillic and syringic acids on the outermost part of wooden piles from La Marmotta site indicates that, before placing the piles in the lake to support the stilt houses, they had been exposed to artificial heating.

3.4. Double-Shot Py(HMDS)-GC/MS

The high chemical complexity of archaeological wood, as emerged in the previous sections, can be further enhanced when wood is treated with consolidating materials, a situation often encountered when waterlogged wood artefacts are displayed in museums. It is common knowledge that consolidating materials, such as polyethylene glycol (PEG), do not terminate the natural degradation of wood and can sometimes accelerate it [106–108]. It is therefore particularly useful to examine the preservation state of archaeological wood in the presence of consolidating agents.

Single-shot Py(HMDS)-GC/MS is not the most suitable approach in these cases, as the pyrograms are very complex and wood pyrolysis products can co-elute with those deriving from the consolidating material. In the case of the Lyon samples, an alternative approach was suggested by the results obtained in the EGA-MS analysis. In particular, for sample Ly-A1, treated with PEG 4000 and disodium sebacate, three regions of thermal degradation were observed, as shown in Figure 9. The first region (up to 350 °C) was found to mainly contain wood pyrolysis products, with a predominance of lignin fragment ions in the mass spectra, which highlighted an advanced state of carbohydrate depletion. The second region (between 350 and 420 °C) corresponded mainly to the thermal degradation of polyethylene glycol (PEG). The last region (above 420 °C) featured fragment ions derived from both PEG and disodium sebacate. PEG and disodium sebacate could thus be partially thermally separated in sample Ly-A1 by EGA-MS.

On the basis of these results, double-shot Py(HMDS)-GC/MS was experimented with, and 320 °C (slightly below 350 °C) was selected as temperature for the first shot and 600 °C for the second shot. Figure 9 reports the corresponding pyrograms. The pyrolytic profile obtained at 320 °C is mainly rich in lignin pyrolysis products and only a few peaks are related to holocellulose fraction with negligible abundance. The pyrolytic profile obtained at 600 °C showed PEG pyrolysis products in groups of n-mers ($n = 1-8$). This example demonstrates that double-shot Py(HMDS)-GC/MS enabled the separation of wood and consolidation material pyrolysis products to be separated in two different chromatographic profiles, leading to less complex data to be analysed. When suitable comparisons with reference materials are performed, this approach can also achieve some preliminary information on the degradation of the consolidation materials.

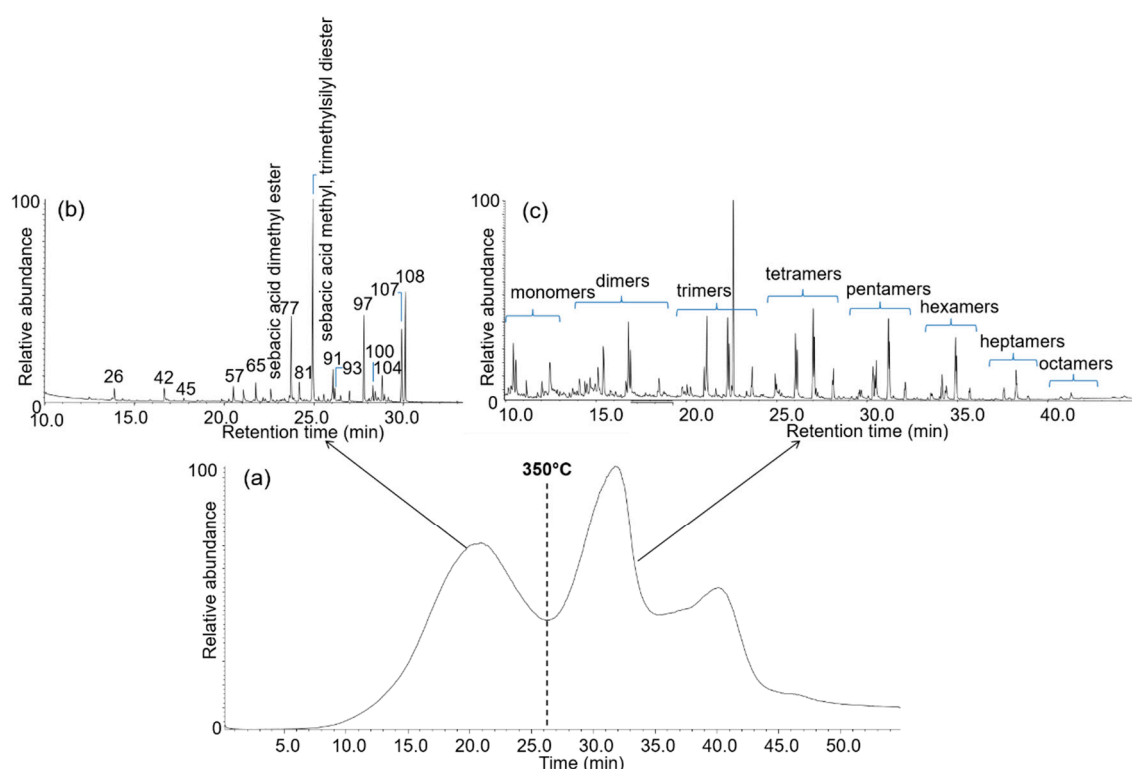


Figure 9. TIT of sample Ly-A1 from the Lyon2 ship obtained by EGA-MS (a) and pyrolytic profiles obtained by double-shot Py(HMDS)-GC/MS of the same sample: first shot at 320 °C (b) and second shot at 600 °C (c), showing the separation between wood and PEG pyrolysis products. Peak labelling refers to Table 3.

4. Conclusions

This review discusses how analytical pyrolysis-based mass spectrometric techniques, such as direct exposure mass spectrometry (DE-MS), evolved gas analysis mass spectrometry (EGA-MS), and single and double-shot pyrolysis gas chromatography mass spectrometry (Py-GC/MS), can be exploited in the study of archaeological lignin and have the ability to provide information on archaeological lignin degradation.

The following main conclusions can be drawn:

- DE-MS facilitates the analysis of a high number of samples in a short time. Differences and similarities between and within wooden samples at a screening level are highlighted by applying principal component analysis (PCA) to the mass spectral data. This method highlights differences in wood degradation pathways, especially in terms of loss of carbohydrates and alteration/depolymerisation/oxidation undergone by lignin.
- EGA-MS facilitates quali-quantitative investigations of wood components in terms of thermo-chemistry, chemical composition, and distribution of pyrolysis products. In addition to the information obtained by the thermographic profiles, the comparison of the relative amounts of lignin pyrolysis products with a carbonyl group at the benzylic position is a powerful approach to highlight the differences in oxidation of both guaiacyl and syringyl lignin. The changes in the relative amounts of lignin dimers are an indication of lignin depolymerisation.
- Single-shot Py(HMDS)-GC/MS provides information on the chemical changes undergone by the residual lignin in archaeological wood, and is fundamental especially when the calculation of the H/L and S/G ratios is not sufficient to highlight differences in the preservation state. The categorisation of lignin pyrolysis products into classes highlights alterations in the side chains of the phenylpropanoid units and oxidation.

Specific degradation products, such as *p*-hydroxybenzoic acid (Oseberg samples) or methyl esters (La Marmotta samples), provide key evidence of the possible causes of lignin degradation in archaeological wood.

- Double-shot Py(HMDS)-GC/MS is a promising approach, which can be applied in combination with EGA-MS to some complex samples containing both wood and consolidating/restoration agents. It reduces the difficulty of interpreting pyrograms containing extremely large numbers of pyrolysis products by producing two simpler chromatograms containing the pyrolysis products of only a fraction of the sample.

Future analytical developments aimed at a better understanding of the chemical composition and degradation of lignin in archaeological objects will entail the integration of Py-GC/MS with other analytical techniques. In particular, the analysis of soluble fractions and oligosaccharides by HPLC-MS, and the development of mass spectrometry methods with high resolution imaging capabilities, are interesting avenues for future research. Finally, integrating mass spectrometric approaches into more holistic multi-analytical investigations that target mechanical and physical properties of archaeological wood is fundamental for the study of composite archaeological objects containing inorganic materials and consolidating agents.

Funding: The study which constituted the basis for this review was performed as a part of the University of Pisa project “PRA_2018_26 Advanced analytical pyrolysis to study polymers in renewable energy, environment, cultural heritage (2018–2020)”, and was also the starting point for the selection of the analytical procedures to be used in the JPI-Cultural Heritage project “STAR—Development of Storage and Assessment methods suited for organic Archaeological artefacts” (2020–2023).

Data Availability Statement: No new data were created or analysed in this study. Data sharing is not applicable to this article.

Conflicts of Interest: The authors declare no conflict of interest.

References

1. Rowell, R.M.; Barbour, R.J. *Archaeological Wood Properties, Chemistry, and Preservation*; Advances in Chemistry Series; American Chemical Society: Washington, DC, USA, 1990.
2. Hedges, J.I. The Chemistry of Archaeological Wood. In *Archaeological Wood*; Rowell, R.M., Barbour, R.J., Eds.; American Chemical Society: Washington, DC, USA, 1990; pp. 111–140.
3. Nilsson, T.; Rowell, R. Historical wood-structure and properties. *J. Cult. Herit.* **2012**, *13*, S5–S9. [[CrossRef](#)]
4. Blanchette, R.A. A review of microbial deterioration found in archaeological wood from different environments. *Int. Biodeterior. Biodegrad.* **2000**, *46*, 189–204. [[CrossRef](#)]
5. Łucejko, J.J.; Mattonai, M.; Zborowska, M.; Tamburini, D.; Cofta, G.; Cantisani, E.; Kúdela, J.; Cartwright, C.; Colombini, M.P.; Ribechini, E.; et al. Deterioration effects of wet environments and brown rot fungus *Contiophora puteana* on pine wood in the archaeological site of Biskupin (Poland). *Microchem. J.* **2018**, *138*, 132–146. [[CrossRef](#)]
6. Singh, A.P. A review of microbial decay types found in wooden objects of cultural heritage recovered from buried and waterlogged environments. *J. Cult. Herit.* **2012**, *13*, S16–S20. [[CrossRef](#)]
7. Tamburini, D.; Łucejko, J.J.; Zborowska, M.; Modugno, F.; Pradzyński, W.; Colombini, M.P. Archaeological wood degradation at the site of Biskupin (Poland): Wet chemical analysis and evaluation of specific Py-GC/MS profiles. *J. Anal. Appl. Pyrolysis* **2015**, *115*, 7–15. [[CrossRef](#)]
8. Braovac, S.; Tamburini, D.; Łucejko, J.J.; McQueen, C.; Kutzke, H.; Colombini, M.P. Chemical analyses of extremely degraded wood using analytical pyrolysis and inductively coupled plasma atomic emission spectroscopy. *Microchem. J.* **2016**, *124*, 368–379. [[CrossRef](#)]
9. Tamburini, D.; Łucejko, J.J.; Pizzo, B.; Mohammed, M.Y.; Sloggett, R.; Colombini, M.P. A critical evaluation of the degradation state of dry archaeological wood from Egypt by SEM, ATR-FTIR, wet chemical analysis and Py(HMDS)-GC-MS. *Polym. Degrad. Stab.* **2017**, *146*, 140–154. [[CrossRef](#)]
10. Łucejko, J.J.; La Nasa, J.; McQueen, C.M.A.; Braovac, S.; Colombini, M.P.; Modugno, F. Protective effect of linseed oil varnish on archaeological wood treated with alum. *Microchem. J.* **2018**, *139*, 50–61. [[CrossRef](#)]
11. Traoré, M.; Kaal, J.; Martínez Cortizas, A. Potential of pyrolysis-GC-MS molecular fingerprint as a proxy of Modern Age Iberian shipwreck wood preservation. *J. Anal. Appl. Pyrolysis* **2017**, *126*, 1–13. [[CrossRef](#)]
12. Braovac, S.; McQueen, C.M.A.; Sahlstedt, M.; Kutzke, H.; Łucejko, J.J.; Klokkernes, T. Navigating conservation strategies: Linking material research on alum-treated wood from the Oseberg collection to conservation decisions. *Herit. Sci.* **2018**, *6*, 77. [[CrossRef](#)]
13. Han, L.; Guo, J.; Wang, K.; Grönquist, P.; Li, R.; Tian, X.; Yin, Y. Hygroscopicity of Waterlogged Archaeological Wood from Xiaobaijiao No.1 Shipwreck Related to Its Deterioration State. *Polym. Adv. Technol.* **2020**, *12*, 834. [[CrossRef](#)]

14. Aluri, E.R.; Reynaud, C.; Bardas, H.; Piva, E.; Cibin, G.; Mosselmans, J.F.W.; Chadwick, A.V.; Schofield, E.J. The Formation of Chemical Degraders during the Conservation of a Wooden Tudor Shipwreck. *ChemPlusChem* **2020**, *85*, 1632–1638. [[CrossRef](#)] [[PubMed](#)]
15. Łucejko, J.J.; Modugno, F.; Ribechini, E.; Tamburini, D.; Colombini, M.P. Analytical instrumental techniques to study archaeological wood degradation. *Appl. Spectrosc. Rev.* **2015**, *50*, 584–625. [[CrossRef](#)]
16. Martín-Seijo, M.; Sartal Lorenzo, M.; Kaal, J.; Teira-Brión, A. A Multi-Disciplinary Study of Woodcrafts and Plant Remains that Reveals the History of Pontevedra's Harbour (Northwest Iberia) Between the 13th and 19th Centuries AD. *Environ. Archaeol.* **2018**, 1–17. [[CrossRef](#)]
17. Guo, J.; Zhang, M.; Liu, J.A.; Luo, R.; Yan, T.; Yang, T.; Jiang, X.; Dong, M.; Yin, Y. Evaluation of the Deterioration State of Archaeological Wooden Artifacts: A Nondestructive Protocol based on Direct Analysis in Real Time—Mass Spectrometry (DART-MS) Coupled to Chemometrics. *Anal. Chem.* **2020**, *92*, 9908–9915. [[CrossRef](#)] [[PubMed](#)]
18. High, K.E.; Penkman, K.E.H. A review of analytical methods for assessing preservation in waterlogged archaeological wood and their application in practice. *Herit. Sci.* **2020**, *8*, 83. [[CrossRef](#)]
19. Dedic, D.; Iversen, T.; Ek, M. Cellulose degradation in the vasa: The role of acids and rust. *Stud. Conserv.* **2013**, *58*, 308–313. [[CrossRef](#)]
20. Bjurhager, I.; Halonen, H.; Lindfors, E.L.; Iversen, T.; Almkvist, G.; Gamstedt, E.K.; Berglund, L.A. State of degradation in archeological oak from the 17th century vasa ship: Substantial strength loss correlates with reduction in (holo)cellulose molecular weight. *Biomacromolecules* **2012**, *13*, 2521–2527. [[CrossRef](#)]
21. Bardet, M.; Gerbaud, G.; Giffard, M.; Doan, C.; Hediger, S.; Le Pape, L. ¹³C High-resolution Solid-State NMR for structural elucidation of archaeological woods. *Prog. Nucl. Magn. Reson. Spectrosc.* **2009**, *55*, 199–214. [[CrossRef](#)]
22. Giachi, G.; Bettazzi, F.; Chimichi, S.; Staccioli, G. Chemical characterisation of degraded wood in ships discovered in a recent excavation of the Etruscan and Roman harbour of Pisa. *J. Cult. Herit.* **2003**, *4*, 75–83. [[CrossRef](#)]
23. Popescu, C.-M.; Popescu, M.-C.; Vasile, C. Structural changes in biodegraded lime wood. *Carbohydr. Polym.* **2010**, *79*, 362–372. [[CrossRef](#)]
24. Macchioni, N.; Pizzo, B.; Capretti, C.; Pecoraro, E.; Sozzi, L.; Lazzeri, S. New Wooden Archaeological Finds from Herculaneum: The State of Preservation and Hypothesis of Consolidation of the Material from the House of the Relief of Telephus. *Archaeometry* **2015**, *58*, 1024–1037. [[CrossRef](#)]
25. Hedges, J.I.; Cowie, G.L.; Ertel, J.R.; James Barbour, R.; Hatcher, P.G. Degradation of carbohydrates and lignins in buried woods. *Geochim. Cosmochim. Acta* **1985**, *49*, 701–711. [[CrossRef](#)]
26. Saiz-Jimenez, C.; de Leeuw, J.W. Pyrolysis-gas chromatography-mass spectrometry of isolated, synthetic and degraded lignins. *Org. Geochem.* **1984**, *6*, 417–422. [[CrossRef](#)]
27. Martínez, A.T.; Camarero, S.; Gutiérrez, A.; Bocchini, P.; Galletti, G.C. Studies on wheat lignin degradation by *Pleurotus* species using analytical pyrolysis. *J. Anal. Appl. Pyrolysis* **2001**, *58*, 401–411. [[CrossRef](#)]
28. van Bergen, P.F.; Poole, I.; Ogilvie, T.M.; Caple, C.; Evershed, R.P. Evidence for demethylation of syringyl moieties in archaeological wood using pyrolysis-gas chromatography/mass spectrometry. *Rapid Commun. Mass Spectrom.* **2000**, *14*, 71–79. [[CrossRef](#)]
29. Pedersen, N.B.; Łucejko, J.J.; Modugno, F.; Björdal, C. Correlation between bacterial decay and chemical changes in waterlogged archaeological wood analysed by light microscopy and Py-GC/MS. *Holzforschung* **2020**. [[CrossRef](#)]
30. Tamburini, D.; Łucejko, J.J.; Modugno, F.; Colombini, M.P. Characterisation of archaeological waterlogged wood from Herculaneum by pyrolysis and mass spectrometry. *Int. Biodeterior. Biodegrad.* **2014**, *86*, 142–149. [[CrossRef](#)]
31. Colombini, M.P.; Łucejko, J.J.; Modugno, F.; Orlandi, M.; Tolppa, E.-L.; Zoia, L. A multi-analytical study of degradation of lignin in archaeological waterlogged wood. *Talanta* **2009**, *80*, 61–70. [[CrossRef](#)]
32. Colombini, M.P.; Orlandi, M.; Modugno, F.; Tolppa, E.-L.; Sardelli, M.; Zoia, L.; Crestini, C. Archaeological wood characterisation by PY/GC/MS, GC/MS, NMR and GPC techniques. *Microchem. J.* **2007**, *85*, 164–173. [[CrossRef](#)]
33. Tamburini, D.; Łucejko, J.J.; Ribechini, E.; Colombini, M.P. Snapshots of lignin oxidation and depolymerization in archaeological wood: An EGA-MS study. *J. Mass Spectrom.* **2015**, *50*, 1103–1113. [[CrossRef](#)] [[PubMed](#)]
34. Łucejko, J.J.; Tamburini, D.; Zborowska, M.; Babiński, L.; Modugno, F.; Colombini, M.P. Oak wood degradation processes induced by the burial environment in the archaeological site of Biskupin (Poland). *Herit. Sci.* **2020**, *8*, 44. [[CrossRef](#)]
35. Łucejko, J.J.; Colombini, M.P.; Ribechini, E. Chemical alteration patterns of ancient Egyptian papyri studied by Pyrolysis-GC/MS with in situ silylation. *J. Anal. Appl. Pyrolysis* **2020**, *152*, 104967. [[CrossRef](#)]
36. Tamburini, D.; Łucejko, J.J.; Modugno, F.; Colombini, M.P. Combined pyrolysis-based techniques to evaluate the state of preservation of archaeological wood in the presence of consolidating agents. *J. Anal. Appl. Pyrolysis* **2016**, *112*, 429–441. [[CrossRef](#)]
37. Łucejko, J.J.; Zborowska, M.; Modugno, F.; Colombini, M.P.; Pradzynski, W. Analytical pyrolysis vs. classical wet chemical analysis to assess the decay of archaeological waterlogged wood. *Anal. Chim. Acta* **2012**, *745*, 70–77. [[CrossRef](#)]
38. Modugno, F.; Ribechini, E.; Calderisi, M.; Giachi, G.; Colombini, M.P. Analysis of lignin from archaeological waterlogged wood by direct exposure mass spectrometry (DE-MS) and PCA evaluation of mass spectral data. *Microchem. J.* **2008**, *88*, 186–193. [[CrossRef](#)]
39. Łucejko, J.J.; Modugno, F.; Colombini, M.P.; Zborowska, M. Archaeological wood from the Wieliczka Salt Mine Museum, Poland—Chemical analysis of wood degradation by Py(HMDS)-GC/MS. *J. Cult. Herit.* **2012**, *13*, S50–S56. [[CrossRef](#)]

40. Zoia, L.; Tamburini, D.; Orlandi, M.; Łucejko, J.J.; Salanti, A.; Tolppa, E.-L.; Modugno, F.; Colombini, M.P. Chemical characterisation of the whole plant cell wall of archaeological wood: An integrated approach. *Anal. Bioanal. Chem.* **2017**, 1–13. [[CrossRef](#)]
41. Traoré, M.; Kaal, J.; Martínez Cortizas, A. FTIR and Py-GC-MS data of wood from various living oak species and Iberian shipwrecks. *Data Brief* **2018**, *21*, 1861–1863. [[CrossRef](#)]
42. Moldoveanu, S.C. *Analytical Pyrolysis of Natural Organic Polymers*; Elsevier Science: Amsterdam, The Netherlands, 1998; Volume 20.
43. Degano, I.; Modugno, F.; Bonaduce, I.; Ribechini, E.; Colombini, M.P. Recent Advances in Analytical Pyrolysis to Investigate Organic Materials in Heritage Science. *Angew. Chem. Int. Ed.* **2018**, *57*, 7313–7323. [[CrossRef](#)]
44. Saiz-Jimenez, C.; de Leeuw, J.W. Lignin pyrolysis products: Their structures and their significance as biomarkers. *Org. Geochem.* **1986**, *10*, 869–876. [[CrossRef](#)]
45. Faix, O.; Meier, D.; Grobe, I. Studies on isolated lignins and lignins in woody materials by pyrolysis-gas chromatography-mass spectrometry and off-line pyrolysis-gas chromatography with flame ionization detection. *J. Anal. Appl. Pyrolysis* **1987**, *11*, 403–416. [[CrossRef](#)]
46. Pouwels, A.D.; Boon, J.J. Analysis of beech wood samples, its milled wood lignin and polysaccharide fractions by curie-point and platinum filament pyrolysis-mass spectrometry. *J. Anal. Appl. Pyrolysis* **1990**, *17*, 97–126. [[CrossRef](#)]
47. Salanti, A.; Zoia, L.; Tolppa, E.L.; Giachi, G.; Orlandi, M. Characterization of waterlogged wood by NMR and GPC techniques. *Microchem. J.* **2010**, *95*, 345–352. [[CrossRef](#)]
48. Oudemans, T.F.M.; Eijkel, G.B.; Boon, J.J. Identifying biomolecular origins of solid organic residues preserved in Iron Age Pottery using DTMS and MVA. *J. Archaeol. Sci.* **2007**, *34*, 173–193. [[CrossRef](#)]
49. Colombini, M.P.; Łucejko, J.; Modugno, F.; Ribechini, E. Characterisation of archaeological waterlogged wood by Direct exposure mass spectrometry (DE-MS) and Pyrolysis/Gas Chromatography/Mass Spectrometry (Py-GC/MS). In Proceedings of the ICOM-WOAM, Amsterdam, The Netherlands, 11–15 September 2007.
50. Colombini, M.P.; Modugno, F.; Ribechini, E. Direct exposure electron ionization mass spectrometry and gas chromatography/mass spectrometry techniques to study organic coatings on archaeological amphorae. *J. Mass Spectrom.* **2005**, *40*, 675–687. [[CrossRef](#)]
51. Modugno, F.; Ribechini, E.; Colombini, M.P. Chemical study of triterpenoid resinous materials in archaeological findings by means of direct exposure electron ionisation mass spectrometry and gas chromatography/mass spectrometry. *Rapid Commun. Mass Spectrom.* **2006**, *20*, 1787–1800. [[CrossRef](#)]
52. van der Hage, E.R.E.; Mulder, M.M.; Boon, J.J. Structural characterization of lignin polymers by temperature-resolved in-source pyrolysis—mass spectrometry and Curie-point pyrolysis—gas chromatography/mass spectrometry. *J. Anal. Appl. Pyrolysis* **1993**, *25*, 149–183. [[CrossRef](#)]
53. Łucejko, J.J. *Waterlogged Archaeological Wood: Chemical Study of Wood Degradation and Evaluation of Consolidation Treatments*; VDM Verlag Dr Muller: Saarbrücken, Germany, 2010.
54. Łucejko, J.J.; Modugno, F.; Ribechini, E.; del Río, J.C. Characterisation of archaeological waterlogged wood by pyrolytic and mass spectrometric techniques. *Anal. Chim. Acta* **2009**, *654*, 26–34. [[CrossRef](#)]
55. Tamburini, D.; Cartwright, C.R.; Gasson, P.; Łucejko, J.J.; Leme, C.L.D. Using analytical pyrolysis and scanning electron microscopy to evaluate charcoal formation of four wood taxa from the caatinga of north-east Brazil. *J. Anal. Appl. Pyrolysis* **2020**, *151*, 104909. [[CrossRef](#)]
56. Nardella, F.; Mattonai, M.; Ribechini, E. Evolved gas analysis-mass spectrometry and isoconversional methods for the estimation of component-specific kinetic data in wood pyrolysis. *J. Anal. Appl. Pyrolysis* **2020**, *145*, 104725. [[CrossRef](#)]
57. Mattonai, M.; Watanabe, A.; Shiono, A.; Ribechini, E. Degradation of wood by UV light: A study by EGA-MS and Py-GC/MS with on line irradiation system. *J. Anal. Appl. Pyrolysis* **2019**, *139*, 224–232. [[CrossRef](#)]
58. Bonaduce, I.; Andreotti, A. Py-GC/MS of Organic Paint Binders. In *Organic Mass Spectrometry in Art and Archeology*; Colombini, M.P., Modugno, F., Eds.; Wiley: Chichester, UK, 2009; pp. 303–326.
59. Challinor, J.M. Review: The development and applications of thermally assisted hydrolysis and methylation reactions. *J. Anal. Appl. Pyrolysis* **2001**, *61*, 3–34. [[CrossRef](#)]
60. Fabbri, D.; Chiavari, G. Analytical pyrolysis of carbohydrates in the presence of hexamethyldisilazane. *Anal. Chim. Acta* **2001**, *449*, 271–280. [[CrossRef](#)]
61. Kuroda, K.-I. Pyrolysis-trimethylsilylation analysis of lignin: Preferential formation of cinnamyl alcohol derivatives. *J. Anal. Appl. Pyrolysis* **2000**, *56*, 79–87. [[CrossRef](#)]
62. Tamburini, D.; Łucejko, J.J.; Ribechini, E.; Colombini, M.P. New markers of natural and anthropogenic chemical alteration of archaeological lignin revealed by in situ pyrolysis/silylation-gas chromatography-mass spectrometry. *J. Anal. Appl. Pyrolysis* **2016**, *118*, 249–258. [[CrossRef](#)]
63. Tamburini, D. From the Burial Environment to the Laboratory: The Analytical Challenge of Archaeological Wood. Ph.D. Thesis, University of Pisa, Pisa, Italy, 2015.
64. Babiński, L.; Fejfer, M.; Prączyński, W. Environmental Monitoring at the Lusatian Culture Settlement in Biskupin, Poland. In *Journal of Wetland Archaeology*; Coles, B., Ed.; Oxbow Books: Oxford, UK, 2007; pp. 51–72.
65. Babiński, L.; Prączyński, W. Ocena warunków zalegania i stopnia degradacji drewna biskupińskiego. Cele i zakres projektu badawczego. In Proceedings of the 22 Sympozjum “Ochrona Drewna”, Warszawa, Poland, 14–16 September 2004; pp. 43–50.

66. Fugazzola Delpino, M.A.; D'Eugenio, G.; Pessina, A. "La Marmotta" (Anguillara Sabazia, RM). Scavi 1989. Un abitato perilacustre di età neolitica. *Bull. Paletnol. Ital.* **1993**, *84*, 181–304.
67. Fugazzola Delpino, M.A. Su alcuni funghi rinvenuti nel villaggio neolitico de "La Marmotta" (Anguillara Sabazia, Roma). Considerazioni preliminari. *Bull. Paletnol. Ital.* **2004**, *95*, 1–20.
68. Bonde, N.; Christensen, A.E. Dendrochronological dating of the Viking Age ship burials at Oseberg, Gokstad and Tune, Norway. *Antiquity* **1993**, *67*, 575–583. [[CrossRef](#)]
69. Brøgger, A.W.; Shetelig, H.; Falk, H. *Osebergfundet*; Distribuert ved Universitetets Oldsaksamling: Oslo, Norway, 1917.
70. McQueen, C.M.A.; Tamburini, D.; Łucejko, J.J.; Braovac, S.; Gambineri, F.; Modugno, F.; Colombini, M.P.; Kutzke, H. New insights into the degradation processes and influence of the conservation treatment in alum-treated wood from the Oseberg collection. *Microchem. J.* **2017**, *132*, 119–129. [[CrossRef](#)]
71. Bruni, S. The urban harbour of Pisae and the wrecks discovered at the Pisa–San Rossore railway station. In *Le Navi Antiche Di Pisa Ad Un Anno Dall'Inizio Delle Ricerche*; Bruni, S., Ed.; Polistampa: Florence, Italy, 2000; pp. 21–79.
72. Eggers, H.J. Die wendischen Burgwälle in Mittelpommern. *Balt. Stud.* **1960**, *47*, 13–46.
73. Kaźmierczak, R.; Niegowski, J. *Sprawozdanie Z Podwodnych Badań Sondażowych Przeprowadzonych Przy Stanowiskach Archeologicznych W Powiatach Drawsko Pomorskie Oraz Szczecinek*; University of Toruń, Instytut of Archaeology: Toruń, Poland, 2003.
74. Chaumat, G.; Blanc, L.; Albino, C. Study of the azelaic/palmitic acids association to treat waterlogged archaeological wood. In Proceedings of the 11th ICOM-CC Group on Wet Organic Archaeological Materials Conference, Greenville, SC, USA, 11–15 October 2010; pp. 207–217.
75. Saiz-Jimenez, C.; Boon, J.J.; Hedges, J.I.; Hessels, J.K.C.; De Leeuw, J.W. Chemical characterization of recent and buried woods by analytical pyrolysis. Comparison of pyrolysis data with ¹³C NMR and wet chemical data. *J. Anal. Appl. Pyrolysis* **1987**, *11*, 437–450. [[CrossRef](#)]
76. Klap, V.A.; Boon, J.J.; Hemminga, M.A.; van Soelen, J. Chemical characterization of lignin preparations of fresh and decomposing *Spartina anglica* by pyrolysis mass spectrometry. *Org. Geochem.* **1998**, *28*, 707–727. [[CrossRef](#)]
77. Faix, O.; Bremer, J.; Meier, D.; Fortmann, I.; Scheijen, M.A.; Boon, J.J. Characterization of tobacco lignin by analytical pyrolysis and Fourier transform-infrared spectroscopy. *J. Anal. Appl. Pyrolysis* **1992**, *22*, 239–259. [[CrossRef](#)]
78. MacKay, J.; Dimmel, D.R.; Boon, J.J. Pyrolysis Mass Spectral Characterization of Wood from Cad-Deficient Pine. *J. Wood Chem. Technol.* **2001**, *21*, 19–29. [[CrossRef](#)]
79. Mulder, M.M.; Pureveen, J.B.M.; Boon, J.J.; Martinez, A.T. An analytical pyrolysis mass spectrometric study of *Eucryphia cordifolia* wood decayed by white-rot and brown-rot fungi. *J. Anal. Appl. Pyrolysis* **1991**, *19*, 175–191. [[CrossRef](#)]
80. van der Hage, E.R.E. Pyrolysis Mass Spectrometry of Lignin Polymers. Ph.D. Thesis, University of Amsterdam, Amsterdam, The Netherlands, 1995.
81. Wold, H. Estimation of principal components and related models by iterative least squares. In *Multivariate Analysis*; Krishnaiah, P., Ed.; Academic Press: New York, NY, USA, 1966; pp. 391–420.
82. Pouwels, A.D.; Eijkel, G.B.; Boon, J.J. Curie-point pyrolysis-capillary gas chromatography-high-resolution mass spectrometry of microcrystalline cellulose. *J. Anal. Appl. Pyrolysis* **1989**, *14*, 237–280. [[CrossRef](#)]
83. Ralph, J.; Hatfield, R.D. Pyrolysis-GC-MS characterization of forage materials. *J. Agric. Food Chem.* **1991**, *39*, 1426–1437. [[CrossRef](#)]
84. Galletti, G.C.; Bocchini, P. Pyrolysis/gas chromatography/mass spectrometry of lignocellulose. *Rapid Commun. Mass Spectrom.* **1995**, *9*, 815–826. [[CrossRef](#)]
85. Alén, R.; Kuoppala, E.; Oesch, P. Formation of the main degradation compound groups from wood and its components during pyrolysis. *J. Anal. Appl. Pyrolysis* **1996**, *36*, 137–148. [[CrossRef](#)]
86. Hosoya, T.; Kawamoto, H.; Saka, S. Cellulose–hemicellulose and cellulose–lignin term interactions in wood pyrolysis at gasification temperature. *J. Anal. Appl. Pyrolysis* **2007**, *80*, 118–125. [[CrossRef](#)]
87. Kotake, T.; Kawamoto, H.; Saka, S. Mechanisms for the formation of monomers and oligomers during the pyrolysis of a softwood lignin. *J. Anal. Appl. Pyrolysis* **2014**, *105*, 309–316. [[CrossRef](#)]
88. Kotake, T.; Kawamoto, H.; Saka, S. Pyrolytic formation of monomers from hardwood lignin as studied from the reactivities of the primary products. *J. Anal. Appl. Pyrolysis* **2015**, *113*, 57–64. [[CrossRef](#)]
89. Shimada, M. Stereobiochemical approach to lignin biodegradation: Possible significance of nonstereospecific oxidation catalyzed by laccase for lignin decomposition by white-rot fungi. In *Lignin Biodegradation: Microbiology, Chemistry, and Potential Applications*; Kirk, T.K., Higuchi, T., Chang, H.-M., Eds.; CRC Press: Boca Raton, FL, USA, 1980.
90. Lourenço, A.; Gominho, J.; Marques, A.V.; Pereira, H. Reactivity of syringyl and guaiacyl lignin units and delignification kinetics in the kraft pulping of *Eucalyptus globulus* wood using Py-GC-MS/FID. *Bioresour. Technol.* **2012**, *123*, 296–302. [[CrossRef](#)]
91. Vinciguerra, V.; Napoli, A.; Bistoni, A.; Petrucci, G.; Sgherzi, R. Wood decay characterization of a naturally infected London plane-tree in urban environment using Py-GC/MS. *J. Anal. Appl. Pyrolysis* **2007**, *78*, 228–231. [[CrossRef](#)]
92. Tamburini, D.; Łucejko, J.J.; Zborowska, M.; Modugno, F.; Cantisani, E.; Mamoňová, M.; Colombini, M.P. The short-term degradation of cellulosic pulp in lake water and peat soil: A multi-analytical study from the micro to the molecular level. *Int. Biodeterior. Biodegrad.* **2017**, *116*, 243–259. [[CrossRef](#)]
93. del Río, J.C.; Gutiérrez, A.; Hernando, M.; Landín, P.; Romero, J.; Martínez, Á.T. Determining the influence of eucalypt lignin composition in paper pulp yield using Py-GC/MS. *J. Anal. Appl. Pyrolysis* **2005**, *74*, 110–115. [[CrossRef](#)]

94. Martínez, Á.T.; Speranza, M.; Ruiz-Dueñas, F.J.; Ferreira, P.; Camarero, S.; Guillén, F.; Martínez, M.J.; Gutiérrez, A.; del Río, J.C. Biodegradation of lignocellulosics: Microbial, chemical, and enzymatic aspects of the fungal attack of lignin. *Int. Microbiol.* **2005**, *8*, 195–204.
95. Lu, R.; Kamiya, Y.; Miyakoshi, T. Applied analysis of lacquer films based on pyrolysis-gas chromatography/mass spectrometry. *Talanta* **2006**, *70*, 370–376. [[CrossRef](#)]
96. Rahimi, A.; Ulbrich, A.; Coon, J.J.; Stahl, S.S. Formic-acid-induced depolymerization of oxidized lignin to aromatics. *Nature* **2014**, *515*, 249–252. [[CrossRef](#)]
97. Tabassum, S.; Sulaiman, O.; Ibrahim, M.; Hashim, R.; Altamash, T. Removal of chemically hazardous p-hydroxybenzoic acid during total chlorine free bleaching process of Hevea Brasiliensis. *J. Clean. Prod.* **2012**, *25*, 68–72. [[CrossRef](#)]
98. Partenheimer, W. The aerobic oxidative cleavage of lignin to produce hydroxy-aromatic benzaldehydes and carboxylic acids via metal/bromide catalysts in acetic/water mixtures. *Adv. Synth. Catal.* **2009**, *351*, 456–466. [[CrossRef](#)]
99. Araújo, J.D.P.; Grande, C.A.; Rodrigues, A.E. Vanillin production from lignin oxidation in a batch reactor. *Chem. Eng. Res. Des.* **2010**, *88*, 1024–1032. [[CrossRef](#)]
100. Ohra-Aho, T.; Tenkanen, M.; Tamminen, T. Direct analysis of lignin and lignin-like components from softwood kraft pulp by Py-GC/MS techniques. *J. Anal. Appl. Pyrolysis* **2005**, *74*, 123–128. [[CrossRef](#)]
101. Prins, M.J.; Ptasinski, K.J.; Janssen, F.J.J.G. Torrefaction of wood: Part 2. Analysis of products. *J. Anal. Appl. Pyrolysis* **2006**, *77*, 35–40. [[CrossRef](#)]
102. Nocquet, T.; Dupont, C.; Commandre, J.-M.; Grateau, M.; Thiery, S.; Salvador, S. Volatile species release during torrefaction of wood and its macromolecular constituents: Part 1—Experimental study. *Energy* **2014**, *72*, 180–187. [[CrossRef](#)]
103. Fernández de Simón, B.; Martínez, J.; Sanz, M.; Cadahía, E.; Esteruelas, E.; Muñoz, A.M. Volatile compounds and sensorial characterisation of red wine aged in cherry, chestnut, false acacia, ash and oak wood barrels. *Food Chem.* **2014**, *147*, 346–356. [[CrossRef](#)]
104. Culleré, L.; Fernández de Simón, B.; Cadahía, E.; Ferreira, V.; Hernández-Orte, P.; Cacho, J. Characterization by gas chromatography–olfactometry of the most odor-active compounds in extracts prepared from acacia, chestnut, cherry, ash and oak woods. *LWT Food Sci. Technol.* **2013**, *53*, 240–248. [[CrossRef](#)]
105. Hernández-Orte, P.; Franco, E.; Huerta, C.G.; García, J.M.; Cabellos, M.; Suberviola, J.; Orriols, I.; Cacho, J. Criteria to discriminate between wines aged in oak barrels and macerated with oak fragments. *Food Res. Int.* **2014**, *57*, 234–241. [[CrossRef](#)]
106. Sandström, M.; Jalilehvand, F.; Persson, I.; Gelius, U.; Frank, P.; Hall-Roth, I. Deterioration of the seventeenth-century warship Vasa by internal formation of sulphuric acid. *Nature* **2002**, *415*, 893–897. [[CrossRef](#)]
107. Preston, J.; Smith, A.D.; Schofield, E.J.; Chadwick, A.V.; Jones, M.A.; Watts, J.E.M. The effects of Mary Rose conservation treatment on iron oxidation processes and microbial communities contributing to acid production in marine archaeological timbers. *PLoS ONE* **2014**, *9*, e84169. [[CrossRef](#)] [[PubMed](#)]
108. Hocker, E.; Almkvist, G.; Sahlstedt, M. The Vasa experience with polyethylene glycol: A conservator’s perspective. *J. Cult. Herit.* **2012**, *13*, S175–S182. [[CrossRef](#)]